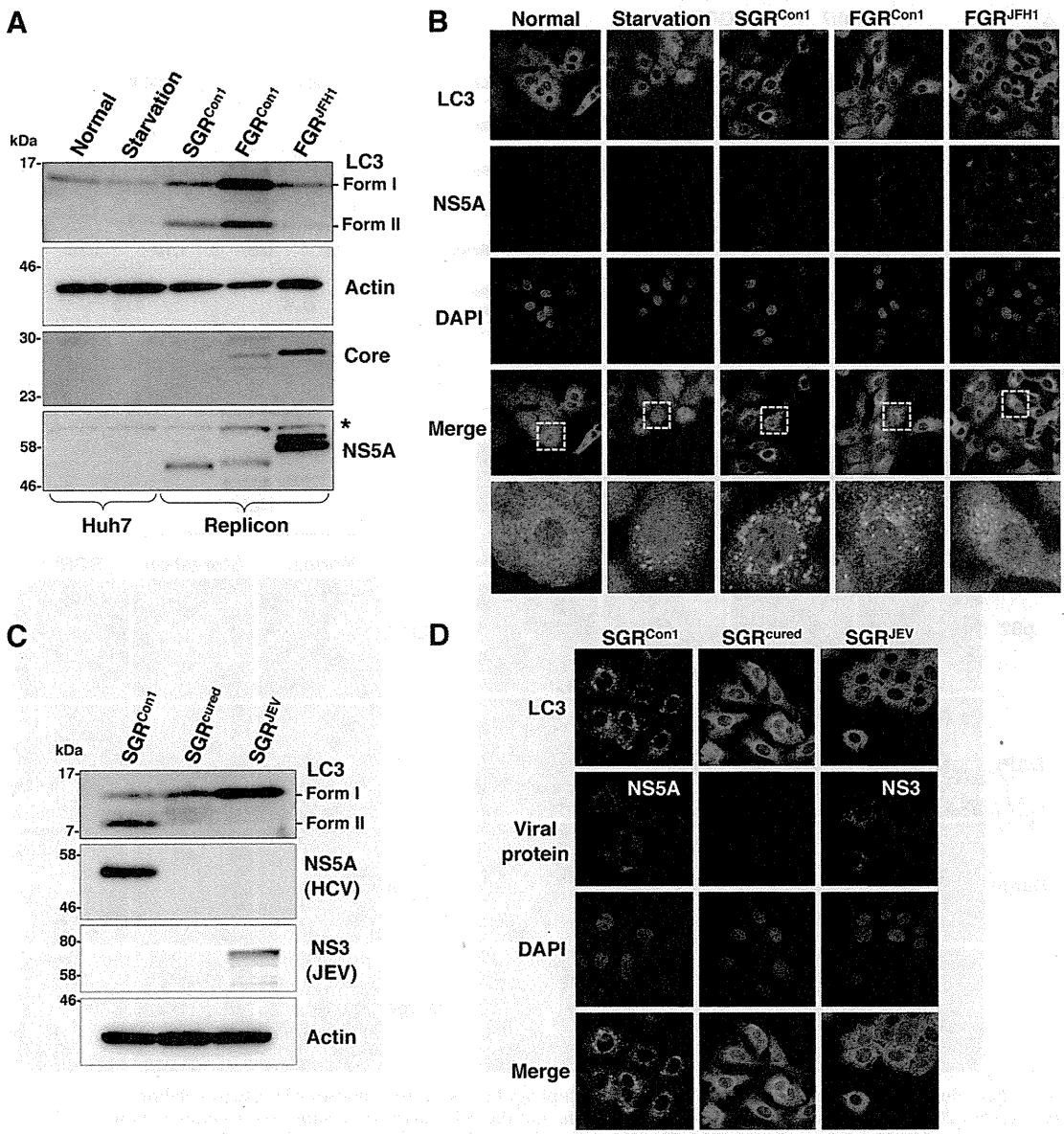

FIG. 1. Induction of autophagy in the HCV replicon cells. (A) The starved Huh7 cells and HCV replicon cells harboring a sub- or full genomic RNA of strain Con1 or strain JFH1 were subjected to immunoblotting using the appropriate antibodies. The asterisk indicates a nonspecific band. (B) Subcellular localizations of LC3 and NS5A were determined by confocal microscopy. The replicon cells and the starved Huh7 cells were stained with DAPI and then reacted with rabbit polyclonal anti-LC3 and mouse monoclonal anti-NS5A antibodies, respectively, followed by Alexa Fluor 488- and 594-conjugated secondary antibodies, respectively. The boxed areas in the merged images are magnified. (C) SGR^{Con1} cells were treated with alpha interferon for 1 week to remove the HCV replicon RNA. The resulting cells were designated SGR^{cured} cells. The SGR^{Con1}, SGR^{cured}, and SGR^{JEV} cells were lysed and subjected to immunoblotting using the appropriate antibodies. (D) Subcellular localization of LC3 and JEV NS3 and HCV NS5A was determined by confocal microscopy after staining with DAPI, followed by staining with rabbit polyclonal anti-LC3 and anti-JEV NS3 antibodies and mouse monoclonal anti-NS5A antibodies and then with the appropriate secondary antibodies. The data shown are representative of three independent experiments.

cells by treatment with the inhibitors, whereas only a slight increase was observed in the SGR^{Con1} cells (5.4-fold versus 1.6-fold) (Fig. 2A), suggesting that autophagy is suppressed in the HCV replicon cells. Furthermore, cytoplasmic accumulation of LC3 was significantly increased in the naïve Huh7 cells by treatment with the inhibitors, in contrast to the only slight increase induced by treatment in the SGR^{Con1} cells (Fig. 2B). In SGR^{Con1} cells, the LC3 foci were colocalized with the polyubiquitin-binding protein p62/SQSTM1, a specific substrate for autophagy (18), suggesting that most of the autophagosomes were distributed in the cytoplasm of the SGR^{Con1} cells (Fig. 2B and C). Next, to examine the autophagy flux in the SGR^{Con1} cells, we monitored the green fluorescent protein (GFP)-conjugated LC3 dynamics in living cells by using time-lapse imaging techniques (see movies in the supplemental material). A large number of small GFP-LC3 foci were detected in the

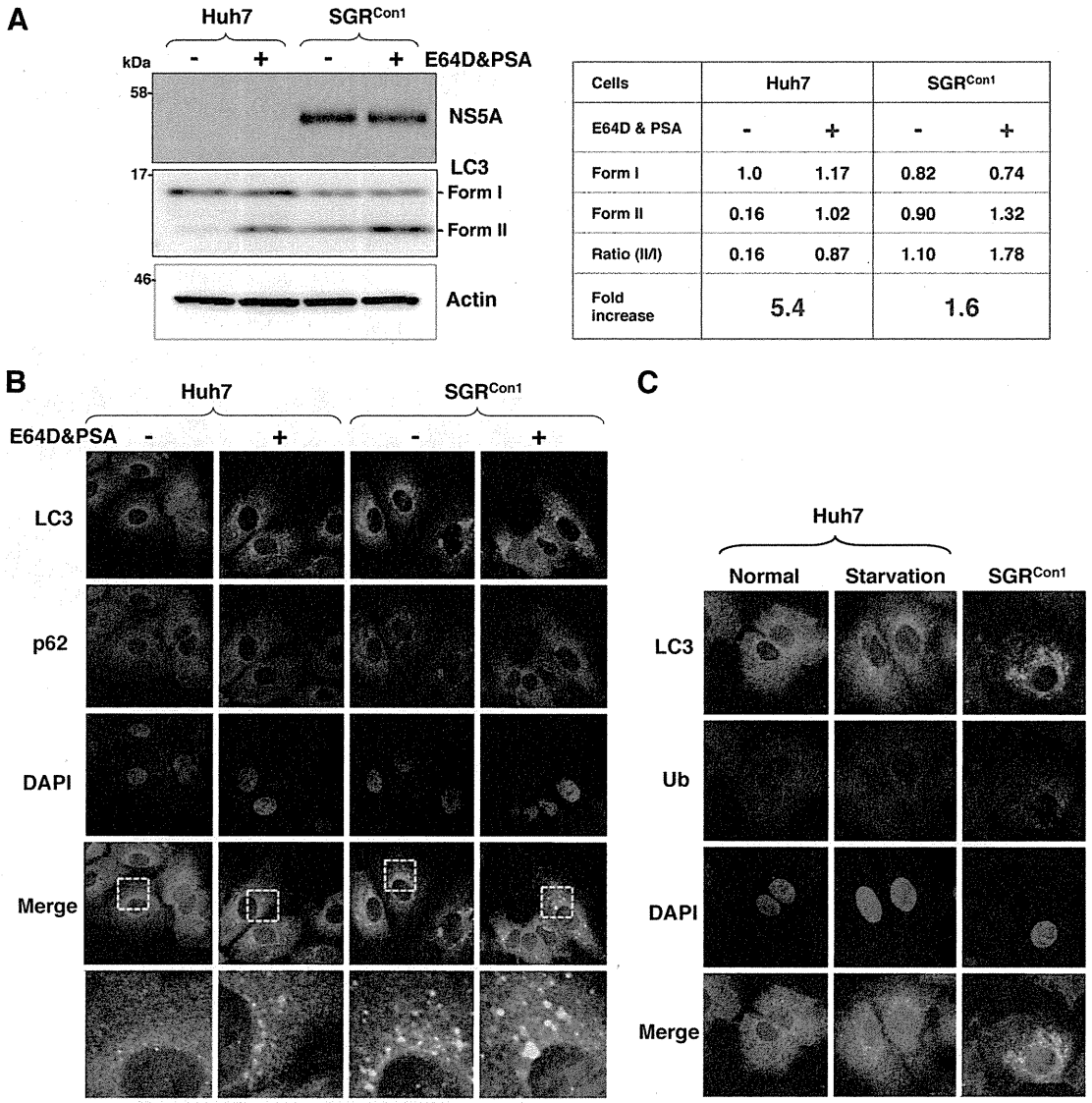

Cells	Huh7		SGR^{Con1}	
E64D & PSA	-	+	-	+
Form I	1.0	1.17	0.82	0.74
Form II	0.16	1.02	0.90	1.32
Ratio (II/I)	0.16	0.87	1.10	1.78
Fold increase	5.4		1.6	

FIG. 2. Autophagy flux is impaired in the HCV replicon cells. Autophagy flux assay using lysosomal protease inhibitors. (A) Huh7 and SGR^{Con1} cells were treated with 20 μM E64D and pepstatin A (PSA) for 6 h, and the cell lysates were subjected to immunoblotting. The density of the protein band was estimated by Multi Gauge version 2.2 (Fujifilm). (B) After nuclear staining with DAPI, the intracellular localizations of LC3 and p62 in each cell were determined by staining with rabbit polyclonal anti-LC3 and mouse monoclonal anti-62 antibodies, respectively, followed by staining with Alexa Fluor 488- and 594-conjugated secondary antibodies, respectively. The resulting cells were observed by confocal microscopy. (C) Colocalization of accumulated LC3 with ubiquitinated proteins (Ub) in SGR^{Con1} cells. Nontreated and starved Huh7 cells and SGR^{Con1} cells were fixed and stained with DAPI and rabbit anti-LC3 and anti-ubiquitin (6C1.17) (BD) polyclonal antibodies, respectively, and then with the appropriate secondary antibodies. Subcellular localizations of LC3 and Ub were determined by confocal microscopy. The data shown are representative of three independent experiments.

starved Huh7 cell, moved quickly, and finally disappeared within 30 min. Although small foci of GFP-LC3 exhibited characteristics similar to those in the starved cells, some large foci exhibited confined movement and maintained constant fluorescence for at least 3 h in the SGR^{Con1} cells. The GFP-LC3 foci in the SGR^{JFH1} cells showed characteristics similar to those in the starved cells. These results support the notion that autophagy flux is suppressed in the SGR^{Con1} cells at some step after autophagosome formation.

Impairment of autolysosomal acidification causes incomplete autophagy in the replicon cell of strain Con1. Recent studies have shown that some viruses inhibit the autophagy pathway by blocking the autolysosome formation (10, 42). Therefore, we determined the autolysosome formation in the HCV replicon cells through the fusion of autophagosome with lysosome. Colocalization of small foci of LC3 with LAMP1, a lysosome marker, was observed in the starved Huh7 cells, SGR^{Con1} cells, and SGR^{JFH1} cells but not in the SGR^{cured} cells (Fig. 3A), suggesting that autolysosomes are formed in the HCV replicon cells of both Con1 and JFH1 strains. The autolysosome is acidified by the vacuolar-type H^+ ATPase (V-ATPase) and degrades substrates by the lysosomal acidic hy-

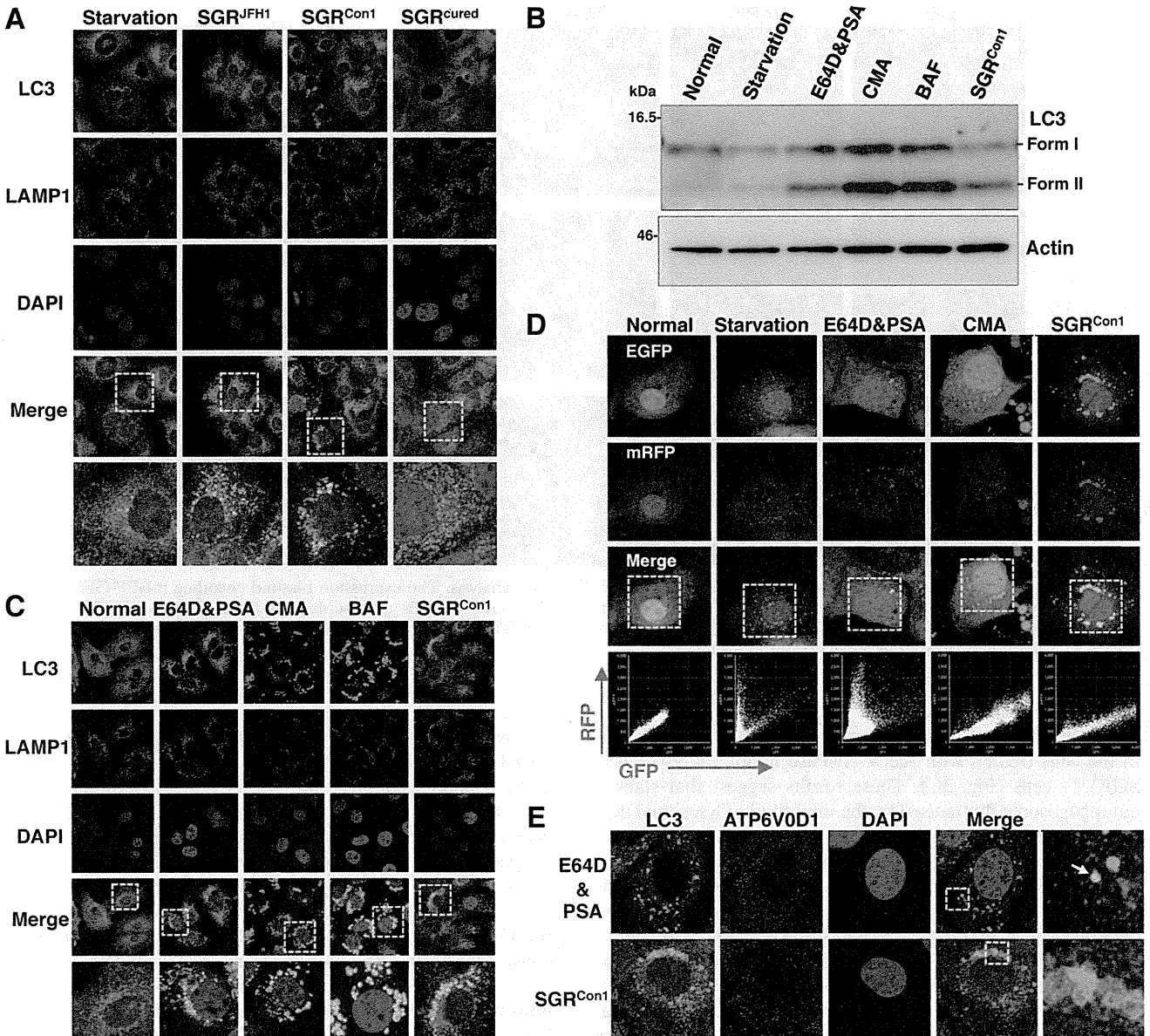

FIG. 3. Inhibition of autophagy maturation in HCV replicon cells. (A) After nuclear staining with DAPI, starved Huh7 cells, replicon cells, and SGR^{cured} cells were stained with rabbit polyclonal anti-LC3 and mouse monoclonal anti-LAMP1 antibodies followed by Alexa Fluor 488- and 594-conjugated secondary antibodies, respectively, and examined by confocal microscopy. The boxed regions in the merged images are magnified. (B and C) Huh7 cells were treated with 20 μM protease inhibitors (E64D and PSA) or a 20 nM concentration of a V-ATPase inhibitor (CMA or BAF) for 6 h. (B) Cell lysates were subjected to immunoblotting using antibodies against LC3 and β-actin. (C) Intracellular localization of LAMP1 and LC3 was determined by confocal microscopy after staining with DAPI and appropriate antibodies. The boxed areas in the merged images are magnified. (D) Tandem fluorescence-tagged LC3 assay. The expression plasmid encoding mRFP-GFP-tandem-tagged LC3 was transfected into naïve and starved Huh7 cells or into the SGR^{Con1} cells treated with the indicated inhibitors at 36 h posttransfection. The resulting cells were fixed at 42 h posttransfection, and the relative GFP and RFP signals were determined by confocal microscopy. The fluorescent values in the boxes of the merged images were determined and shown as dot plots in the bottom column of the grid, in which the *x* and *y* axes indicate the signals of GFP and RFP, respectively. (E) Huh7 cells treated with E64D and PSA and the SGR^{Con1} cells were stained with DAPI and then with rabbit polyclonal anti-LC3 and mouse monoclonal anti-ATP6V0D1 antibodies followed by Alexa Fluor 488- and 594-conjugated secondary antibodies, respectively. The boxed regions in the merged images are magnified. A white arrow indicates colocalization of LC3 and ATP6V0D1. The data shown are representative of three independent experiments.

drolases in the vesicle (2). Next, to determine the possibility of a deficiency in the acidification of the autolysosome on the autophagic dysfunction in the Con1 replicon cells, Huh7 cells were treated with the protease inhibitors E64D and pepstatin A (PSA) or with each of the V-ATPase inhibitors concanamycin A (CMA) and bafilomycin A1 (BAF). The amount of LC3-II was significantly increased in Huh7 cells treated with the inhibitors just as in the SGR^{Con1} cells (Fig. 3B). Further-

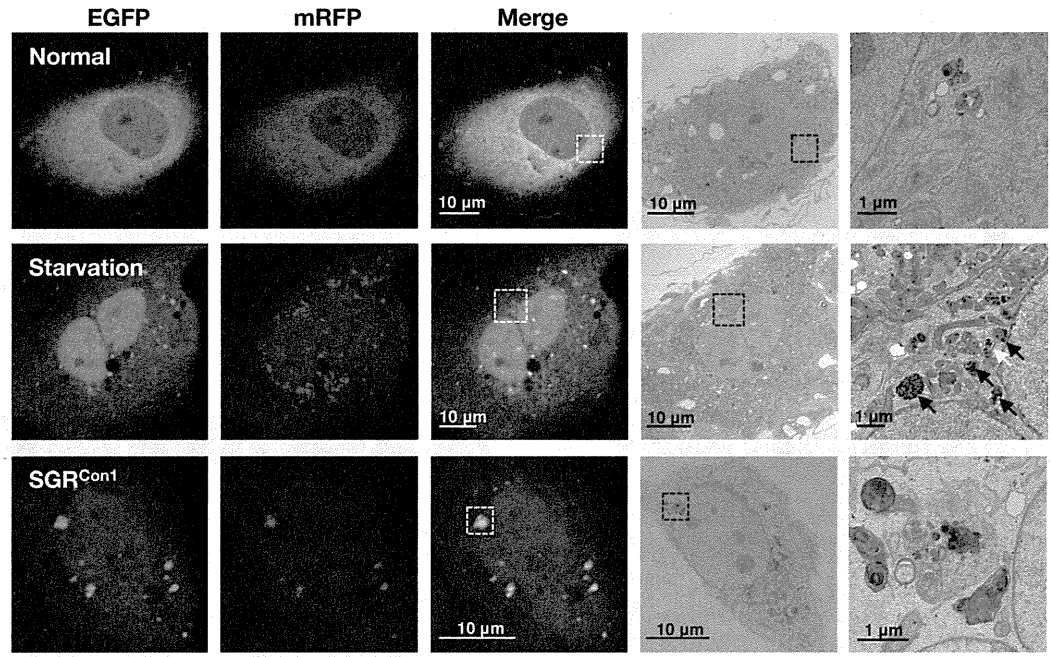

FIG. 4. Correlative fluorescence microscopy-electron microscopy (FM-EM) analysis. The expression plasmid encoding mRFP-GFP-tandem-tagged LC3 was transfected into naïve and starved Huh7 cells or into the SGR^{Con1} cells as described in the legend to Fig. 3D, and the mRFP-GFP-tandem-tagged LC3 signals were observed at 36 h posttransfection. The boxed regions in the merged images are magnified. The data shown are representative of three independent experiments.

more, the large foci of LC3 colocalized with LAMP1 appeared in the cells treated with the V-ATPase inhibitors, as seen in SGR^{Con1} cells (Fig. 3C). These results suggest that stacked autophagosome flux caused by the inhibition of lysosomal degradation or acidification exhibits characteristics similar to those observed in the Con1 replicon cells.

Since the fluorescence of GFP but not that of monomeric red fluorescent protein (mRFP) disappears under the acidic environment, expression of mRFP-GFP tandem fluorescent-tagged LC3 (tfLC3) is capable of being used to monitor the acidic status of the autolysosome (24). Both GFP and mRFP fluorescent signals were unfused, some of them accumulated as small foci in Huh7 cells after starvation or by treatment with the protease inhibitors, and half of the foci of mRFP were not colocalized with those of GFP (Fig. 3D), indicating that half of the foci are in an acidic state due to maturation into an autolysosome after fusion with a lysosome. On the other hand, the large foci of GFP and mRFP were completely colocalized in Huh7 cells treated with CMA or in the SGR^{Con1} cells. These results suggest that the large foci of LC3 in the SGR^{Con1} cells are not under acidic conditions. Recently, it was shown that the lack of lysosomal acidification in human genetic disorders due to dysfunction in assembly/sorting of V-ATPase induces incomplete autophagy similar to that observed in SGR^{Con1} cells (31, 45). Therefore, to explore the reason for the lack of acidification of the autolysosome in the SGR^{Con1} cells, we examined the subcellular localization of ATP6V0D1, a subunit of the integral membrane V_0 complex of V-ATPase. Colocalization of ATP6V0D1 with large foci of LC3 was observed in Huh7 cells treated with the protease inhibitors but not in SGR^{Con1} cells (Fig. 3E), suggesting that dislocation of V-ATPase may participate in the impairment of the autolysosomal acidification in the SGR^{Con1} cells.

We further examined the morphological characteristics of the LC3-positive compartments by using correlative fluorescence microscopy-electron microscopy (FM-EM) (Fig. 4). The starved Huh7 cells exhibited a small double-membrane vesicle (white arrow) and high-density single-membrane structures (black arrows) in close proximity to the correlative position of the GFP- and mRFP-positive LC3 compartments, which are considered to be the autophagosome and lysosome/autolysosome, respectively. In contrast, many high-density membranous structures were detected in the correlative position of the large GFP- and mRFP-positive LC3 compartment in the SGR^{Con1} cells, which is well consistent with the observation in the time-lapse imaging in which small foci of LC3 headed toward and assembled with the large LC3-positive compartment (see movies in the supplemental material). These results suggest that the formation of large aggregates with aberrant inner structures in the SGR^{Con1} cells may impair maturation of the autolysosome through the interference of further fusion with functional lysosomes for the degradation.

The secretion of immature cathepsin B is enhanced in the replicon cell of strain Con1. Lysosomal acidification is required for the cleavage of cathepsins for activation, and cathepsin B (CTSB) is processed under acidic conditions (13). Although a marginal decrease of CTSB was detected in the whole lysates of the SGR^{Con1} cells, a significant reduction in the expression of both unprocessed (pro-CTSB) and matured CTSB was observed in the lysosomal fractions of the SGR^{Con1} cells compared with those of the naïve Huh7 and the SGR^{cured} cells (Fig. 5A). LAMP1 was concentrated at a similar level in

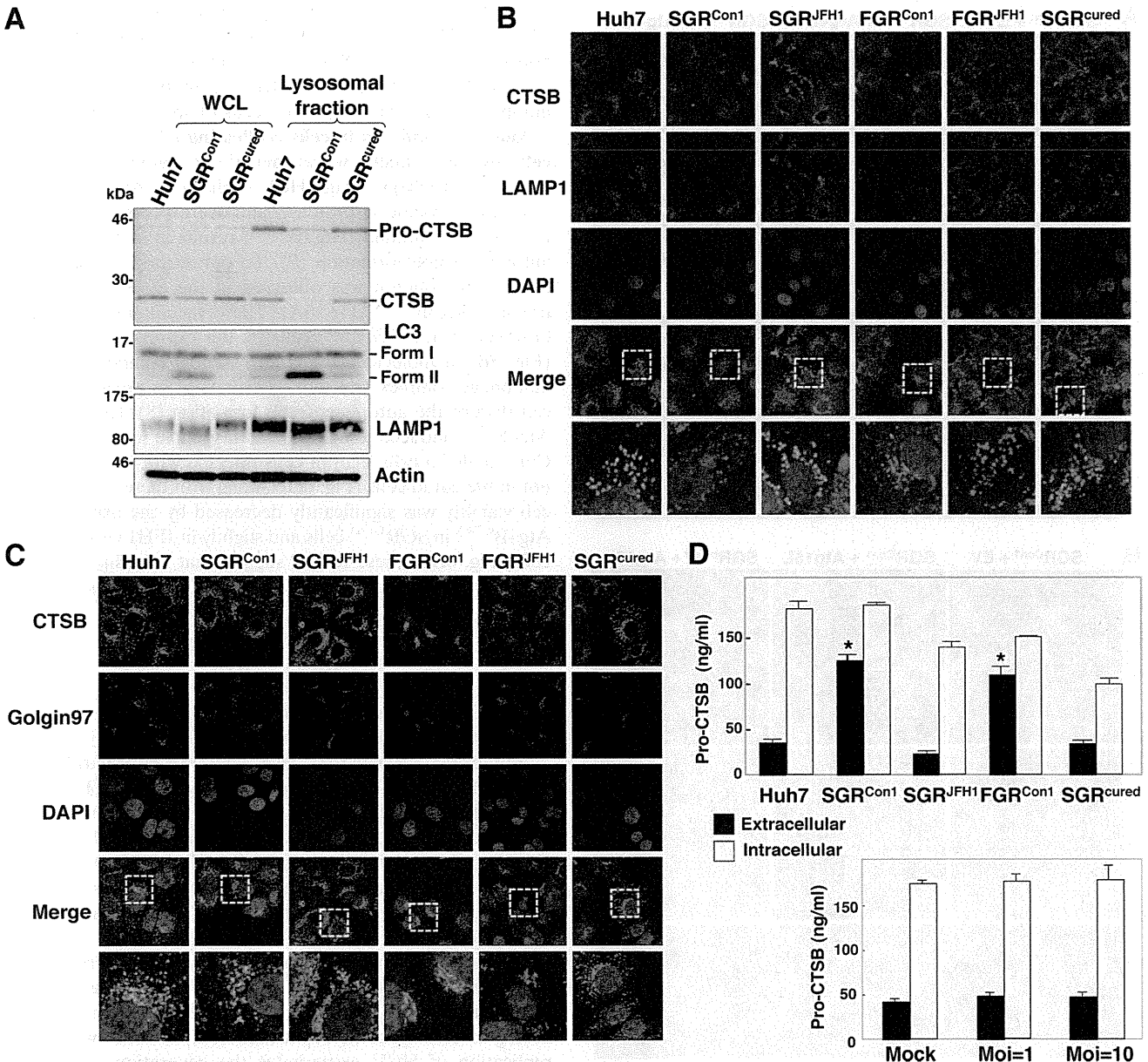

FIG. 5. Enhanced secretion of pro-CTSB in the HCV replicon cells. (A) The whole-cell lysate (WCL) and lysosomal fraction prepared from Huh7, SGR^{Con1}, and SGR^{cured} cells were subjected to immunoblotting. (B and C) Huh7 cells, HCV replicon cells, and SGR^{cured} cells were stained with DAPI, rabbit polyclonal anti-CTSB antibody, and mouse anti-LAMP1 (B) or anti-Golgin97 (C) antibody. The boxed areas in the merged images are magnified. (D) Expression of pro-cathepsin B in the culture supernatants (black bars) and cell lysates (white bars) of the Huh7, SGR^{Con1}, SGR^{JFH1}, FGR^{Con1}, and SGR^{cured} cells and the SGR^{cured} cells infected with HCVcc at a multiplicity of infection (Moi) of 1 or 10 and incubated for 72 h was determined by enzyme-linked immunosorbent assay (ELISA). The error bars indicate standard deviations. The asterisks indicate significant differences ($P < 0.01$) versus the control value. The data shown are representative of three independent experiments.

the lysosomal fractions of the cells, whereas LC-II was detected in the fractions of the SGR^{Con1} cells but not in those of Huh7 and the SGR^{cured} cells, suggesting that autophagosomes and/or autolysosomes in the SGR^{Con1} cells are fractionated in the lysosomal fraction. Colocalization of CTSB with LAMP1 was observed in the naïve Huh7 cells, in the SGR^{cured} cells, and in the replicon cells harboring a sub- or a full genomic RNA of strain JFH1 (SGR^{JFH1} and FGR^{JFH1}, respectively) but not in those of strain Con1 (SGR^{Con1} and FGR^{Con1}) (Fig. 5B). On the other hand, CTSB was colocalized with Golgin97, a marker for the Golgi apparatus, in the SGR^{Con1} and FGR^{Con1} cells but not in other cells (Fig. 5C). Since previous reports suggested that the alkalization in the lysosome triggers secretion of the unprocessed lysosomal enzymes (19, 41), we next determined the secretion of pro-CTSB in the replicon cells. Secretion of the pro-CTSB was significantly enhanced in the replicon cells of strain Con1 but not in those of strain JFH1 and naïve and cured cells (Fig. 5D, top). Furthermore, secretion of pro-CTSB

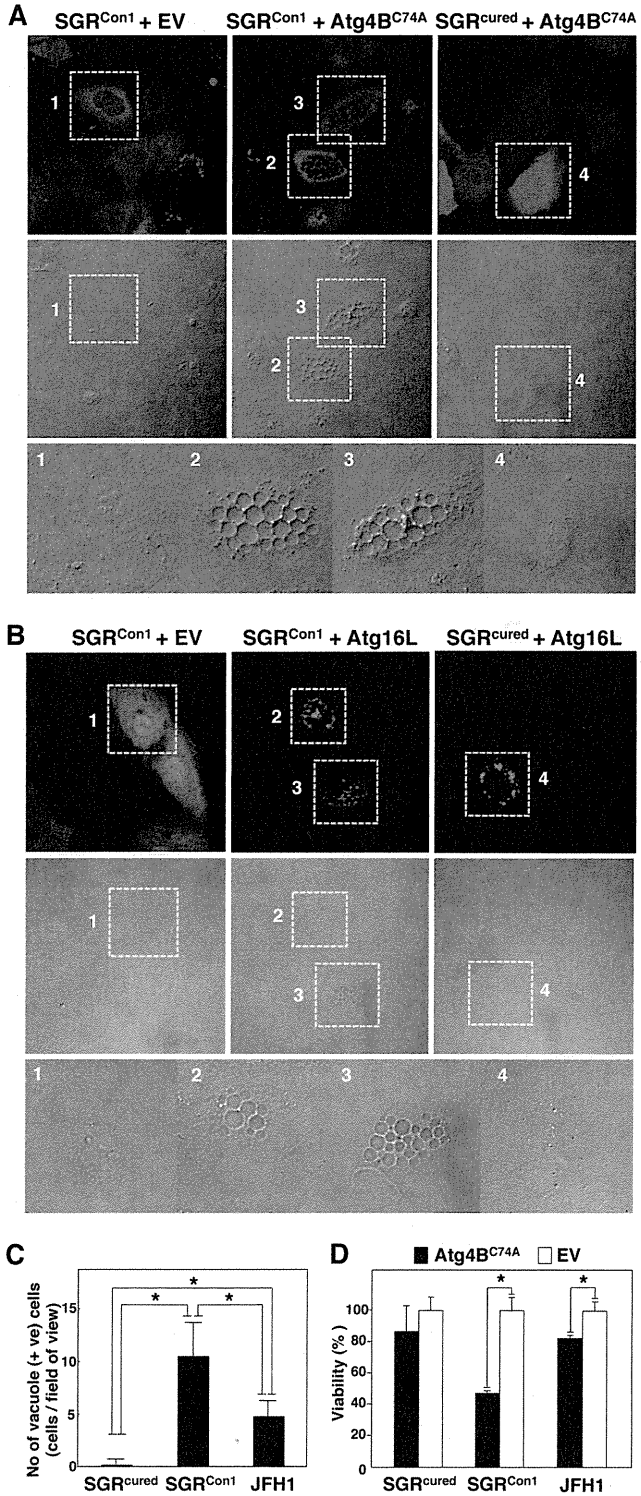

FIG. 6. Inhibition of autophagosome formation induces severe cytoplasmic vacuolations leading to cell death in the HCV replicon cells. (A) SGR^{Con1} and SGR^{cured} cells transfected with pStrawberry-$Atg4B^{C74A}$ or empty vector pStrawberry (EV) were fixed at 48 h posttransfection and examined by fluorescence microscopy. The boxed areas in the phase-contrast images are magnified. (B) SGR^{Con1} and SGR^{cured} cells transfected with pEGFP-Atg16L or EV were examined by fluorescence microscopy at 48 h posttransfection. The boxed areas in the phase-contrast images are magnified. (C) SGR^{cured}, SGR^{Con1}, and SGR^{cured} cells infected with JFH1 virus were transfected with pStrawberry-$Atg4B^{C74A}$, and the number of vacuole-positive cells in each of nine fields of view was counted at 48 h posttransfection. (D) SGR^{cured}, SGR^{Con1}, and SGR^{cured} cells infected with JFH1 virus were transfected with pStrawberry-$Atg4B^{C74A}$ (black bars) or EV (white bars), and cell viability was determined at 6 days posttransfection by using CellTiter-Glo (Promega) according to the manufacturer's protocol. The asterisks indicate significant differences ($P < 0.05$) versus the control value. The data shown are representative of three independent experiments.

was not observed in the cured cells infected with HCVcc, an infectious HCV strain derived from strain JFH1 (Fig. 5D, bottom). Collectively, these results suggest that the dysfunction of lysosomal acidification contributes to the impairment of autophagy in the HCV replicon cells of strain Con1.

Autophagy induced in cells replicating HCV is required for cell survival. Finally, we examined the pathological significance of autophagy during HCV replication. Atg4B is known as an LC3-processing protease, and overexpression of its protease-inactive mutant ($Atg4B^{C74A}$) results in inhibition of the autophagosome formation (7). To our surprise, severe cytoplasmic vacuolation was observed in the SGR^{Con1} cells expressing $Atg4B^{C74A}$ (Fig. 6A). These vacuolations were also observed in the SGR^{Con1} cells by the expression of Atg16L (Fig. 6B), a molecule that is an essential component of the autophagy complex and that, if expressed in excess amounts, can disrupt the autophagosome formation (8). Expression of $Atg4B^{C74A}$ induced a higher level of vacuole formation in the Con1 replicon cells than in cells infected with JFH1 virus but not in the cured cells (Fig. 6C). Along with these vacuolations, cell viability was significantly decreased by the expression of $Atg4B^{C74A}$ in SGR^{Con1} cells and slightly in JFH1 virus-infected cells (Fig. 6D). These results suggest that autophagy induced by the RNA replication of HCV is required for host cell survival.

DISCUSSION

In the present study, we demonstrated that two genotypes of HCV induce autophagy, whereas intact autophagy flux is required for the host cell to survive. The cell death characterized by cytoplasmic vacuolation that was induced in the HCV replicon cells by the inhibition of the autophagosome formation is similar to type III programmed cell death, which is distinguishable from apoptosis and autophagic cell death (4). Type III programmed cell death has been observed in the neurodegenerative diseases caused by the deposit of cytotoxic protein aggregates (15).

We previously reported that HCV hijacks chaperone complexes, which regulates quality control of proteins into the membranous web for circumventing unfolded protein response during efficient genome replication (53); in other words, the replication of HCV exacerbates the generation of proteins associated with cytotoxicity. In the experiments using a chimpanzee model, HCV of genotype 1 was successfully used to reproduce acute and chronic hepatitis similar to that in the human patients (3, 57), and transgenic mice expressing viral proteins of HCV of genotype 1b have been shown to develop

Sjögren syndrome, insulin resistance, hepatic steatosis, and hepatocellular carcinoma (27, 28). In contrast, HCVcc, based on the genotype 2a strain JFH1 isolated from a patient with fulminant hepatitis C (33, 56), was unable to establish chronic infection in chimpanzees (56) or to induce cell damage and inflammation in chimeric mice xenotransplanted with human hepatocytes (17). These results imply that the onset of HCV pathogenesis could be dependent not only upon an amount but also on a property of deposited proteins, and they might explain the aggravated vacuolations under the inhibition of autophagosome formation in strain Con1 compared to that in strain JFH1. Interestingly, the overexpression of $Atg4B^{C74A}$ or Atg16L causes eccentric cell death in the Con1 replicon cells in which autophagy flux is already disturbed. Thus, we speculated that the quarantine of undefined abnormalities endowed with high cytotoxicity by the engulfing of the autophagic membrane might be sufficient for the amelioration of HCV-induced degeneration. The autophagosomal dysfunction observed in the Con1 replicon cells may suggest that a replicant of strain Con1 was more sensitive to the lysosomal vacuolation than that of strain JFH1. Because a limitation of our study was that we were unable to use infectious HCV of other strains, it is still unclear whether the autophagic degradation can be impaired only in the replicon of HCV strain Con1 or genotype 1.

We also demonstrated that HCV replication of strain Con1 but not that of strain JFH1 facilitates the secretion of pro-CTSB. It has been well established that the secretion of pro-CTSB is enhanced in several types of tumors (26, 50). The secretion of CTSB, like the secretion of matrix metalloproteases, is a marker of the progression of the proteolytic degradation of the extracellular matrix, which plays an important part in cancer invasion and metastasis. Since infection with HCV of genotype 1 is clinically considered a risk factor for the development of hepatocellular carcinoma (14, 51), the enhanced secretion of pro-CTSB by the replication of genotype 1 strains might synergistically promote infiltration of hepatocellular carcinoma.

As shown elsewhere (see movies in the supplemental material), although most degradations of the autophagosome were impaired due to a dislocalization of a V-ATPase subunit, some autophagic degradation was achieved in the SGR^{Con1} cells similar to that in the starved Huh7 cells. Moreover, the stagnated autophagy flux was rescued by the treatment of alpha interferon accompanied by elimination of HCV (Fig. 1C and D). Interestingly, we observed neither a significant impairment of lysosomal degradation nor the intracellular activity of cathepsins in the replicon cells of HCV strain Con1 (data not shown). Therefore, there might be a specific dysfunction within the autolysosome during the replication of HCV strain Con1. Detailed studies are needed to elucidate how HCV strain Con1 disturbs the sorting of V-ATPase.

A close relationship between autophagy and the immune system has been gradually unveiled (47). Autophagy assists not only in the direct elimination of pathogens by hydrolytic degradation but also in antigen processing in antigen-presenting cells such as macrophage and dendritic cells (DC) for presentation by major histocompatibility complex (MHC) I and II (11). Moreover, autophagy plays important roles in T lymphocyte homeostasis (44). As such, in some instances, interruptions of autophagy can allow microorganisms to escape from the host immune system. Indeed, the immune response against herpes simplex virus was suppressed by blocking the autophagy (6). With regard to HCV, functionally impaired DC dysfunctions marked by poor DC maturation, impaired antigen presentation, and attenuated cytokine production have been reported in tissue culture models and chronic hepatitis C patients (1, 22, 46). In addition, reduction of cell surface expression of MHC-I in HCV genotype 1b replicon cells has been reported (55). We confirmed that levels of cell surface expression of MHC-I in the replicon cells of genotype 1b, but not of genotype 2a, were reduced in comparison with those in the cured cells (data not shown). Hence it might be feasible to speculate that the replication of HCV RNA of genotype 1 induces an incomplete autophagy for attenuating antigen presentation to establish persistent infection. In contrast, autophagy is known to serve as a negative regulator of innate immunity (21, 54). A recent report demonstrated that autophagy induced by infection with strain JFH1 or dengue virus attenuates innate immunity to promote viral replication (23), indicating that an HCV genotype 2a strain may facilitate autophagy to evade innate immunity.

In this study, we demonstrated that HCV utilizes autophagy to circumvent the cell death induced by vacuole formation for its survival. This unique strategy of HCV propagation may provide new clues to the virus-host interaction and, ultimately, to the pathogenesis of infection by various genotypes of HCV.

ACKNOWLEDGMENTS

We thank H. Murase and M. Tomiyama for their secretarial work. We also thank R. Bartenschlager and T. Wakita for providing cell lines and plasmids.

This work was supported in part by grants-in-aid from the Ministry of Health, Labor, and Welfare (Research on Hepatitis), the Ministry of Education, Culture, Sports, Science, and Technology, and the Osaka University Global Center of Excellence Program.

REFERENCES

1. **Auffermann-Gretzinger, S., E. B. Keeffe, and S. Levy.** 2001. Impaired dendritic cell maturation in patients with chronic, but not resolved, hepatitis C virus infection. Blood **97:**3171–3176.
2. **Beyenbach, K. W., and H. Wieczorek.** 2006. The V-type H+ ATPase: molecular structure and function, physiological roles and regulation. J. Exp. Biol. **209:**577–589.
3. **Bradley, D. W.** 2000. Studies of non-A, non-B hepatitis and characterization of the hepatitis C virus in chimpanzees. Curr. Top. Microbiol. Immunol. **242:**1–23.
4. **Clarke, P. G.** 1990. Developmental cell death: morphological diversity and multiple mechanisms. Anat. Embryol. (Berl.) **181:**195–213.
5. **Dreux, M., P. Gastaminza, S. F. Wieland, and F. V. Chisari.** 2009. The autophagy machinery is required to initiate hepatitis C virus replication. Proc. Natl. Acad. Sci. U. S. A. **106:**14046–14051.
6. **English, L., et al.** 2009. Autophagy enhances the presentation of endogenous viral antigens on MHC class I molecules during HSV-1 infection. Nat. Immunol. **10:**480–487.
7. **Fujita, N., et al.** 2008. An Atg4B mutant hampers the lipidation of LC3 paralogues and causes defects in autophagosome closure. Mol. Biol. Cell **19:**4651–4659.
8. **Fujita, N., et al.** 2008. The Atg16L complex specifies the site of LC3 lipidation for membrane biogenesis in autophagy. Mol. Biol. Cell **19:**2092–2100.
9. **Fujitani, Y., C. Ebato, T. Uchida, R. Kawamori, and H. Watada.** 2009. β-cell autophagy: a novel mechanism regulating β-cell function and mass: lessons from β-cell-specific Atg7-deficient mice. Islets **1:**151–153.
10. **Gannage, M., et al.** 2009. Matrix protein 2 of influenza A virus blocks autophagosome fusion with lysosomes. Cell Host Microbe **6:**367–380.
11. **Gannage, M., and C. Munz.** 2009. Autophagy in MHC class II presentation of endogenous antigens. Curr. Top. Microbiol. Immunol. **335:**123–140.
12. **Hara, T., et al.** 2006. Suppression of basal autophagy in neural cells causes neurodegenerative disease in mice. Nature **441:**885–889.
13. **Hasilik, A.** 1992. The early and late processing of lysosomal enzymes: proteolysis and compartmentation. Experientia **48:**130–151.

14. **Hatzakis, A., et al.** 1996. Hepatitis C virus 1b is the dominant genotype in HCV-related carcinogenesis: a case-control study. Int. J. Cancer **68:**51–53.
15. **Hirabayashi, M., et al.** 2001. VCP/p97 in abnormal protein aggregates, cytoplasmic vacuoles, and cell death, phenotypes relevant to neurodegeneration. Cell Death Differ. **8:**977–984.
16. **Hiraga, N., et al.** 2011. Rapid emergence of telaprevir resistant hepatitis C virus strain from wildtype clone in vivo. Hepatology (Baltimore, Md.) **54:** 781–788.
17. **Hiraga, N., et al.** 2007. Infection of human hepatocyte chimeric mouse with genetically engineered hepatitis C virus and its susceptibility to interferon. FEBS Lett. **581:**1983–1987.
18. **Ichimura, Y., E. Kominami, K. Tanaka, and M. Komatsu.** 2008. Selective turnover of p62/A170/SQSTM1 by autophagy. Autophagy **4:**1063–1066.
19. **Isidoro, C., et al.** 1995. Altered intracellular processing and enhanced secretion of procathepsin D in a highly deviated rat hepatoma. Int. J. Cancer **60:**61–64.
20. **Jacobson, I. M., P. Cacoub, L. Dal Maso, S. A. Harrison, and Z. M. Younossi.** 2010. Manifestations of chronic hepatitis C virus infection beyond the liver. Clin. Gastroenterol. Hepatol. **8:**1017–1029.
21. **Jounai, N., et al.** 2007. The Atg5 Atg12 conjugate associates with innate antiviral immune responses. Proc. Natl. Acad. Sci. U. S. A. **104:**14050–14055.
22. **Kanto, T., et al.** 1999. Impaired allostimulatory capacity of peripheral blood dendritic cells recovered from hepatitis C virus-infected individuals. J. Immunol. **162:**5584–5591.
23. **Ke, P. Y., and S. S. Chen.** 2011. Activation of the unfolded protein response and autophagy after hepatitis C virus infection suppresses innate antiviral immunity in vitro. J. Clin. Invest. **121:**37–56.
24. **Kimura, S., N. Fujita, T. Noda, and T. Yoshimori.** 2009. Monitoring autophagy in mammalian cultured cells through the dynamics of LC3. Methods Enzymol. **452:**1–12.
25. **Kiyosawa, K., et al.** 1990. Interrelationship of blood transfusion, non-A, non-B hepatitis and hepatocellular carcinoma: analysis by detection of antibody to hepatitis C virus. Hepatology **12:**671–675.
26. **Koblinski, J. E., et al.** 2002. Interaction of human breast fibroblasts with collagen I increases secretion of procathepsin B. J. Biol. Chem. **277:**32220–32227.
27. **Koike, K., et al.** 1997. Sialadenitis histologically resembling Sjogren syndrome in mice transgenic for hepatitis C virus envelope genes. Proc. Natl. Acad. Sci. U. S. A. **94:**233–236.
28. **Koike, K., T. Tsutsumi, H. Yotsuyanagi, and K. Moriya.** 2010. Lipid metabolism and liver disease in hepatitis C viral infection. Oncology **78**(Suppl. 1)**:**24–30.
29. **Komatsu, M., et al.** 2006. Loss of autophagy in the central nervous system causes neurodegeneration in mice. Nature **441:**880–884.
30. **Komatsu, M., et al.** 2007. Homeostatic levels of p62 control cytoplasmic inclusion body formation in autophagy-deficient mice. Cell **131:**1149–1163.
31. **Lee, J. H., et al.** 2010. Lysosomal proteolysis and autophagy require presenilin 1 and are disrupted by Alzheimer-related PS1 mutations. Cell **141:** 1146–1158.
32. **Levine, B., and G. Kroemer.** 2008. Autophagy in the pathogenesis of disease. Cell **132:**27–42.
33. **Lindenbach, B. D., et al.** 2005. Complete replication of hepatitis C virus in cell culture. Science **309:**623–626.
34. **Lohmann, V., et al.** 1999. Replication of subgenomic hepatitis C virus RNAs in a hepatoma cell line. Science **285:**110–113.
35. **Manns, M. P., et al.** 2001. Peginterferon alfa-2b plus ribavirin compared with interferon alfa-2b plus ribavirin for initial treatment of chronic hepatitis C: a randomised trial. Lancet **358:**958–965.
36. **McHutchison, J. G., et al.** 2009. Telaprevir with peginterferon and ribavirin for chronic HCV genotype 1 infection. N. Engl. J. Med. **360:**1827–1838.
37. **Mizushima, N.** 2007. Autophagy: process and function. Genes Dev. **21:**2861–2873.
38. **Moradpour, D., F. Penin, and C. M. Rice.** 2007. Replication of hepatitis C virus. Nat. Rev. Microbiol. **5:**453–463.
39. **Moriishi, K., and Y. Matsuura.** 2007. Host factors involved in the replication of hepatitis C virus. Rev. Med. Virol. **17:**343–354.
40. **Moriishi, K., and Y. Matsuura.** 2003. Mechanisms of hepatitis C virus infection. Antivir. Chem. Chemother. **14:**285–297.
41. **Oda, K., Y. Nishimura, Y. Ikehara, and K. Kato.** 1991. Bafilomycin A1 inhibits the targeting of lysosomal acid hydrolases in cultured hepatocytes. Biochem. Biophys. Res. Commun. **178:**369–377.
42. **Orvedahl, A., et al.** 2007. HSV-1 ICP34.5 confers neurovirulence by targeting the Beclin 1 autophagy protein. Cell Host Microbe **1:**23–35.
43. **Poordad, F., et al.** 2011. Boceprevir for untreated chronic HCV genotype 1 infection. N. Engl. J. Med. **364:**1195–1206.
44. **Pua, H. H., I. Dzhagalov, M. Chuck, N. Mizushima, and Y. W. He.** 2007. A critical role for the autophagy gene Atg5 in T cell survival and proliferation. J. Exp. Med. **204:**25–31.
45. **Ramachandran, N., et al.** 2009. VMA21 deficiency causes an autophagic myopathy by compromising V-ATPase activity and lysosomal acidification. Cell **137:**235–246.
46. **Saito, K., et al.** 2008. Hepatitis C virus inhibits cell surface expression of HLA-DR, prevents dendritic cell maturation, and induces interleukin-10 production. J. Virol. **82:**3320–3328.
47. **Schmid, D., and C. Munz.** 2007. Innate and adaptive immunity through autophagy. Immunity **27:**11–21.
48. **Schutte, K., J. Bornschein, and P. Malfertheiner.** 2009. Hepatocellular carcinoma—epidemiological trends and risk factors. Dig. Dis. **27:**80–92.
49. **Sir, D., et al.** 2008. Induction of incomplete autophagic response by hepatitis C virus via the unfolded protein response. Hepatology **48:**1054–1061.
50. **Sloane, B. F., et al.** 2005. Cathepsin B and tumor proteolysis: contribution of the tumor microenvironment. Semin. Cancer Biol. **15:**149–157.
51. **Stankovic-Djordjevic, D., et al.** 2007. Hepatitis C virus genotypes and the development of hepatocellular carcinoma. J. Dig. Dis. **8:**42–47.
52. **Strader, D. B., T. Wright, D. L. Thomas, and L. B. Seeff.** 2004. Diagnosis, management, and treatment of hepatitis C. Hepatology **39:**1147–1171.
53. **Taguwa, S., et al.** 2009. Cochaperone activity of human butyrate-induced transcript 1 facilitates hepatitis C virus replication through an Hsp90-dependent pathway. J. Virol. **83:**10427–10436.
54. **Tal, M. C., et al.** 2009. Absence of autophagy results in reactive oxygen species-dependent amplification of RLR signaling. Proc. Natl. Acad. Sci. U. S. A. **106:**2770–2775.
55. **Tardif, K. D., and A. Siddiqui.** 2003. Cell surface expression of major histocompatibility complex class I molecules is reduced in hepatitis C virus subgenomic replicon-expressing cells. J. Virol. **77:**11644–11650.
56. **Wakita, T., et al.** 2005. Production of infectious hepatitis C virus in tissue culture from a cloned viral genome. Nat. Med. **11:**791–796.
57. **Walker, C. M.** 1997. Comparative features of hepatitis C virus infection in humans and chimpanzees. Springer Semin. Immunopathol. **19:**85–98.
58. **Wasley, A., and M. J. Alter.** 2000. Epidemiology of hepatitis C: geographic differences and temporal trends. Semin. Liver Dis. **20:**1–16.
59. **Wong, J., et al.** 2008. Autophagosome supports coxsackievirus B3 replication in host cells. J. Virol. **82:**9143–9153.
60. **Yoshimori, T., and T. Noda.** 2008. Toward unraveling membrane biogenesis in mammalian autophagy. Curr. Opin. Cell Biol. **20:**401–407.

Biochemical and Biophysical Research Communications 411 (2011) 826–831

Contents lists available at ScienceDirect

journal homepage: www.elsevier.com/locate/ybbrc

MicroRNA-22 and microRNA-140 suppress NF- B activity by regulating the expression of NF- B coactivators

Akemi Takata, Motoyuki Otsuka *, Kentaro Kojima, Takeshi Yoshikawa, Takahiro Kishikawa, Haruhiko Yoshida, Kazuhiko Koike

Department of Gastroenterology, Graduate School of Medicine, The University of Tokyo, Tokyo 113-8655, Japan

ARTICLE INFO

Article history:
Received 5 July 2011
Available online 21 July 2011

Keywords:
NF-κB
MicroRNA
NCOA1
NRIP1

ABSTRACT

Nuclear factor κB (NF-κB) is a transcription factor that regulates a set of genes that are critical to many biological phenomena, including liver tumorigenesis. To identify microRNAs (miRNAs) that regulate NF-κB activity in the liver, we screened 60 miRNAs expressed in hepatocytes for their ability to modulate NF-κB activity. We found that miRNA-22 and miRNA-140-3p significantly suppressed NF-κB activity by regulating the expression of nuclear receptor coactivator 1 (NCOA1) and nuclear receptor-interacting protein 1 (NRIP1), both of which are NF-κB coactivators. Our results provide new information about the roles of miRNAs in the regulation of NF-κB activity.

1. Introduction

Nuclear factor κB (NF-κB) is a transcription factor that regulates a set of genes that are critical to immunity, cell proliferation, inflammation, and tumorigenesis [1,2]. NF-κB is composed of homo- or heterodimeric complexes of members of the Rel family of proteins, which consists of p65 (RelA), c-Rel, RelB, p50, and p52. These proteins each contain a Rel homology domain, which mediates dimerization and DNA binding. Two mammalian NF-κB proteins, p105 and p100, have long C-terminal domains that inhibit their activity until they are activated [1]. In canonical NF-κB signaling, p105 is constitutively processed by the proteasome into an active p50 subunit. However, p50 is sequestered in the cytoplasm as a heterodimer, mainly with p65, as a result of its interaction with inhibitory IκB proteins. IκB proteins are phosphorylated by an IKK complex and are degraded, which allows the p50 heterodimer to translocate to the nucleus and activate transcription. In the non-canonical pathway, p100 is only processed to active p52 when the NIK–IKK pathway is activated. Active p52 activates transcription when associated with its binding partner, RelB [1,3]. Canonical and non-canonical NF-κB pathways activate a set of target genes [3].

NF-κB-dependent transcription of target genes requires multiple transcriptional coactivators that probably function by linking sequence-specific activators to the basal transcriptional machinery and/or altering chromatin structure [4]. Such coactivators, which are reported to play critical roles in NF-κB-dependent transcription, include CBP [5], nuclear receptor coactivator-1 (NCOA-1) [6], TIF-2/GRIP-1/NCoA-2 [4], and p/CAF [4].

MicroRNAs (miRNAs) are short, single-stranded, non-coding RNAs. First identified in *Caenorhabditis elegans* [7], they are now known to be expressed in most organisms, ranging from plants to vertebrates [8]. Primary miRNAs, which possess stem-loop structures, are processed into mature miRNAs by Drosha and Dicer RNA polymerase III. These mature miRNAs then associate with the RNA-induced silencing complex (RISC), and the resulting complex directly binds to the 3′-untranslated regions (3′-UTRs) of target mRNAs to suppress translation and gene expression. Different miRNAs are responsible for the control of various biological processes, including cell proliferation, apoptosis, differentiation, metabolism, oncogenesis, and oncogenic suppression [9–11]. In this context, a number of miRNAs have recently been shown to regulate the function of intracellular signaling intermediates, including p53 and NF-κB, by regulating the expression of their target genes [12–14].

The aim of this study was to determine the possible role of miRNAs in NF-κB signaling. We focused on miRNAs expressed in the liver because NF-κB activation plays a crucial role in human liver tumorigenesis [15,16]. To this end, we screened a subset of miRNAs that are expressed in the liver for their ability to modulate NF-κB activity and identified the target genes of miRNAs that may affect NF-κB activity.

1.1. Methods

1.1.1. Cell culture

HepG2, Huh7, PLC/PRF/5, and 293T cells were maintained in Dulbecco's modified Eagle's medium (DMEM) supplemented with 10% fetal bovine serum (FBS).

* Corresponding author. Address: Department of Gastroenterology, Graduate School of Medicine, The University of Tokyo, 5-3-1 Hongo, Bunkyo-ku, Tokyo 113-8655, Japan. Fax: +81 3 3814 0021.
E-mail address: otsukamo-tky@umin.ac.jp (M. Otsuka).

0006-291X/$ - see front matter © 2011 Elsevier Inc. All rights reserved.
doi:10.1016/j.bbrc.2011.07.048

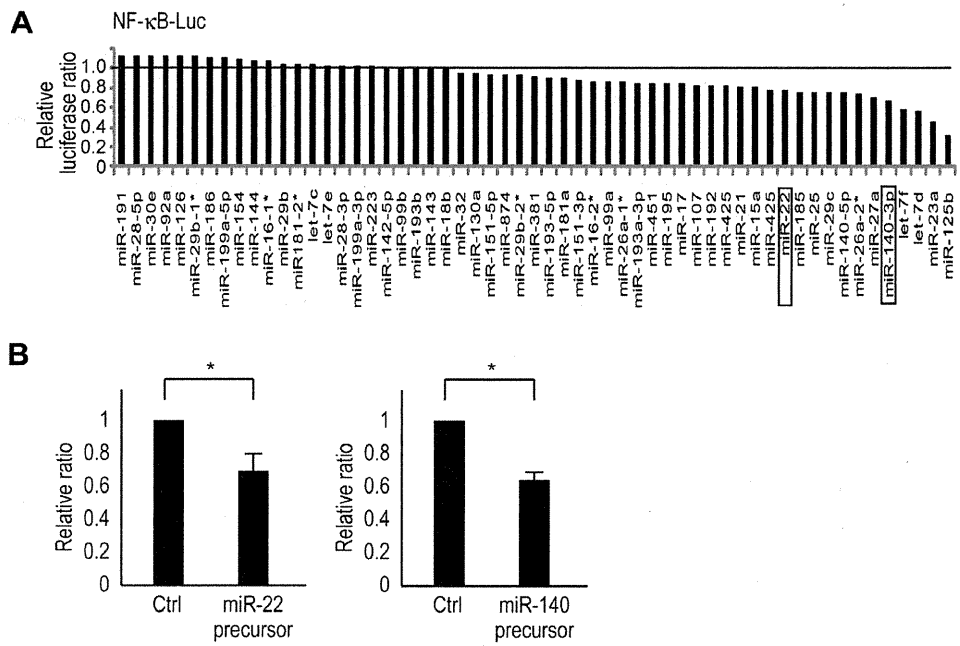

Fig. 1. MiR-22 and miR-140 suppress NF-κB activity. (A) Functional screening for liver miRNAs that modulate NF-κB activity. Sixty mature miRNA oligonucleotides known to be highly expressed in the liver were transiently reverse-transfected into stable 293T cell-derived NF-κB reporter cell lines. Reporter activity values were normalized to the values from negative control RNA oligonucleotides and ranked in descending order. The experiments were performed in duplicate, and the result of a representative trial is shown. The miRNAs in rectangles showed reproducible results. (B) Overexpression of the selected miRNA precursors suppresses NF-κB activity following TNF-α stimulation. NF-κB reporter plasmids were transiently transfected, with or without selected miRNA precursor-expressing plasmids, into HepG2 cells. Relative luciferase activity was measured 24 h after transfection. Values were normalized to those from cells transfected with a miRNA precursor-non-expressing control vector, which were set to 1. $^*p < 0.05$. Data represent the mean ± s.d. of three independent experiments. Similar results were obtained using Huh7 and PLC/PRF/5 cells.

1.1.2. miRNA screening and the establishment of stable reporter cell lines

To establish NF-κB-luc reporter cell lines, 293T cells were transfected with the reporter plasmid pNF-κB-luc (Clontech, Mountain View, CA), which carries a linear hygromycin resistance marker. Single clones were selected in the presence of 250 μg/mL hygromycin. To screen for miRNAs that modulate NF-κB activity, 60 miRNAs that are highly expressed in the liver [17] were selected. Synthetic mature miRNAs and, as a negative control, double-stranded RNA with artificial sequences (B-Bridge, Sapporo, Japan) were applied, with transfection reagents, to 96-well plates. The reporter cells were seeded to the plates, reverse-transfected, and then incubated for 48 h. NF-κB activity was measured after exposure to human recombinant TNF-α (5 ng/mL) for 6 h. The experiments were performed in duplicate, and the data generated were normalized to the values obtained from the negative controls.

1.2. Plasmids

Plasmids expressing miRNA precursors (miR-22, miR-140, and miR-122 precursors) were purchased from System Biosciences (Mountain View, CA). NRIP1-expressing plasmids were purchased from Open Biosystems (Huntsville, AL). Reporter plasmids used to analyze miRNA function were constructed by inserting annealed synthetic primers containing two tandem sequences complementary to each miRNA into the 3′-UTR of the firefly luciferase gene, driven by a CMV promoter (pGL3-basic; Promega, Madison, WI), at the *Fse*I site. The sequences of the primers used were as follows: miR-22, 5′-ACA GTT CTT CAA CTG GCA GCT TAA TTA CAG TTC TTC AAC TGG CAG CTT CTC GAG CCG G-3′; miR-140-3p, 5′-CCG TGG TTC TAC CCT GTG GTA AAT TCC GTG GTT CTA CCC TGT GGT ACT CGA GCC GG-3′; and miR-140-5p, 5′-CTA CCA TAG GGT AAA ACC ACT GAA TTC TAC CAT AGG GTA AAA CCA CTG CTC GAG CCG G-3′. To construct reporter plasmids carrying fragments of the NRIP1 or NCOA1 gene downstream of a CMV-driven firefly luciferase cassette, 450-bp fragments of the NRIP1 or NCOA1 gene 3′-UTR were amplified using human genomic DNA as a template (primers for NRIP1: forward, 5′-GGC CGG CCC AAT GTG TCT GTC CCA C-3′ and reverse, 5′-GGC CGG CCA CTT AGC AGA GAT TCT TG-3′; primers for NCOA1: forward, 5′-GGC CGG CCA GTC ATT GGC TTC TTA TCT GG-3′ and reverse, 5′-GGC CGG CCA AAC TGT ATT TTT TGG ATT TC-3′). The resulting PCR products were cloned into the *Fse*I site of the pGL4.50 vector (Promega). A reporter construct with two point mutations in the seed sequences of the putative miR140-3p target sites was created through site-directed mutagenesis using a Quick Change II site-directed mutagenesis kit (Stratagene, Heidelberg, Germany) according to the manufacturer's instructions. The pNF-κB-luc and pAP-1-luc reporter plasmids, which contain the *Photinus pyralis* (firefly) luciferase reporter gene driven by a basic promoter element (TATA box) and inducible *cis*-enhancer elements, were purchased from Stratagene (La Jolla, CA). To construct a reporter plasmid containing mutated NF-κB-binding sites, the GGGAATTTCC NF-κB binding motifs in pNF-κB-luc were mutated to ATCAATTTCA, as previously described [18]. Briefly, synthetic oligonucleotides with four mutant binding sites (forward, 5′-CTA GCA TCA ATT TCA ATC AAT TTC AAT CAA TTT CAA TCA ATT TCA A-3′; reverse, 5′-GAT CTT GAA ATT GAT TGA AAT TGA TTG AAA TTG ATT GAA ATT GAT G-3′) were annealed and cloned into the *Nhe*I and *Bgl*II sites of pNF-κB-luc to replace the original NF-κB-binding motifs.

1.3. Transfection and luciferase assay

Transfection was performed using FuGene6 Transfection Reagent (Boehringer Mannheim, Mannheim, Germany), according to

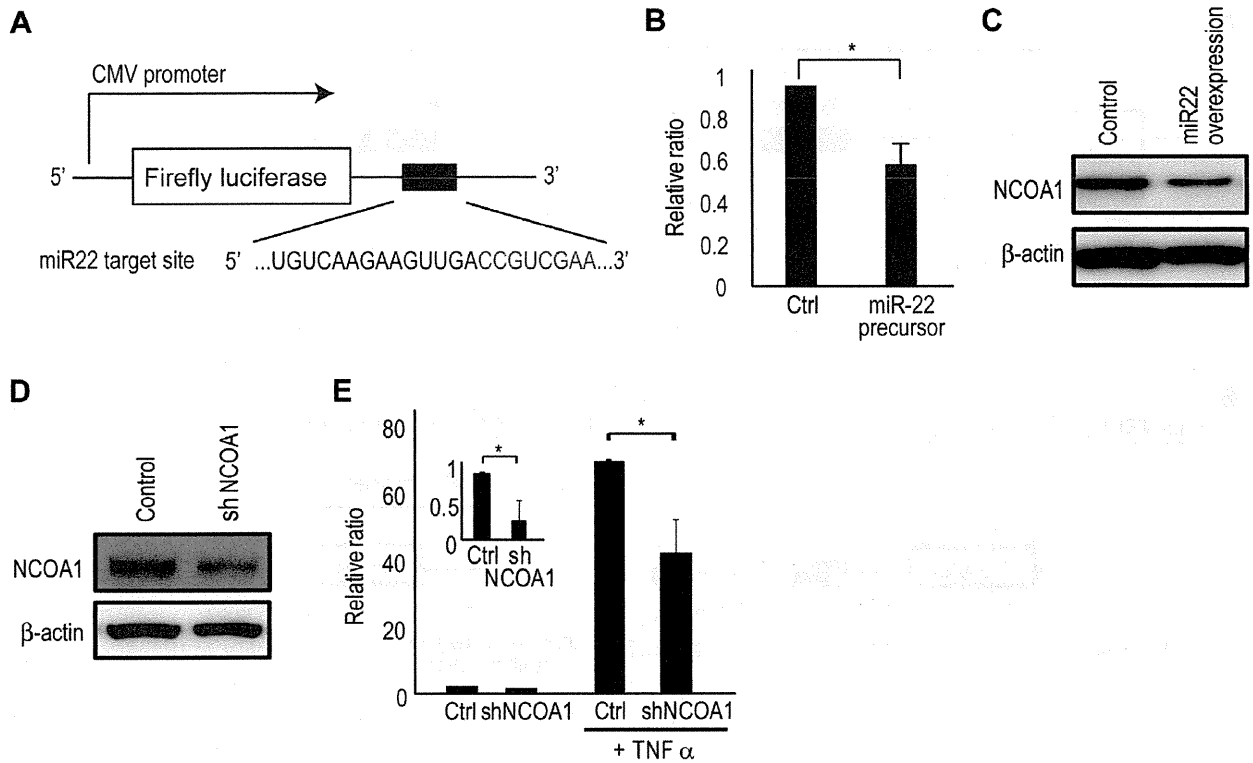

Fig. 2. MiR-22 targets the NF-κB coactivator NCOA1. (A) A luciferase reporter carrying the region of the NCOA1 3′-UTR that contains the putative miR-22 target site was used to assess the effects of miR-22 on NCOA1 expression. The "seed sequences" are shown in red. (B) The NCOA1 3′-UTR was directly targeted by miR-22. Huh7 cells were co-transfected with Luc-NCOA1-3′-UTR and either a control vector or an miR-22 precursor-expressing plasmid for 48 h, and luciferase assays were performed. Data represent the mean ± s.d. of three independent experiments. (C) Overexpression of miR-22 reduces NCOA1 expression. Huh7 cells were infected with miR-22 precursor-expressing lentiviruses. Whole-cell lysates were analyzed by Western blotting using an anti-NCOA1 antibody. Values represent protein levels normalized to the β-actin signal. A result representative of three independent experiments is shown. (D) Confirmation of NCOA1 knockdown in Huh7 cells infected with NCOA1 shRNA-expressing lentiviral particles. (E) Knockdown of NCOA1 reduced NF-κB activation. NF-κB reporter activity was reduced in NCOA1-knockdown Huh7 cells. Data represent the mean ± s.d. of three independent experiments (inset, results from cells not treated with TNF-α). Similar results were obtained using PLC/PRF/5 cells.

the manufacturer's instructions. pRL-TK, a control plasmid containing *Renilla reniformis* (sea pansy) luciferase, driven by the herpes simplex virus thymidine kinase promoter (Toyo Ink, Tokyo, Japan), was used as an internal control. Cells were harvested 48 h after transfection, and luciferase assays were performed as described previously [19]. In some cases, NF-κB activity was measured after exposure to human recombinant TNF-α (5 ng/mL) for 6 h.

1.4. Lentiviral production and transduction

RIP140 (NRIP1)-shRNA and NCOA1-shRNA lentiviral particles were purchased from Santa Cruz Biotechnology (Santa Cruz, CA). To produce miR-22- or miR-140-expressing lentiviruses, 293T cells were transfected with pPACKH1 Packaging Plasmid Mix (System Biosciences) and pCDH-miR22- or pCDH-miR140-expressing lentivector constructs. After 2 days, the supernatants were collected and the viruses were concentrated using PEG-it Virus Precipitation Solution (System Biosciences), according to the manufacturer's recommended protocol. Cells were transduced with lentiviral particles and then selected using puromycin.

1.5. Antibodies

The following antibodies were used for Western blotting: rabbit anti-RIP140 (NRIP1) (R5027) and mouse anti-β-actin (A5316), purchased from Sigma (St. Louis, MO); and rabbit anti-NCOA1 (SRC-1) (#2191), purchased from Cell Signaling Technology (Danvers, MA).

1.6. Western blotting

Cell extract protein concentrations were measured using a DC Protein Assay Kit (Bio-Rad, Hercules, CA). Thirty micrograms of total protein were resolved, and Western Blotting was performed as described previously [20].

1.7. Statistical analysis

Statistically significant differences between groups were determined using Student's *t*-test, when variances were equal. When variances were unequal, Welch's *t*-test was instead used.

2. Results

2.1. miR-22 and miR-140 suppress NF-κB activity

Because some miRNAs regulate important intracellular signaling pathways [12,14,21], we initially screened for miRNAs that affect NF-κB activity, using stable NF-κB activity reporter cell lines and by transiently overexpressing 60 kinds of mature synthetic miRNAs. Because we were interested in the function of liver miRNAs [19], the miRNAs examined were selected on the basis of their expression in the liver [22]. We used non-liver 293T cells intentionally. The screening revealed differential effects of miRNAs on NF-κB activity in response to TNF-α stimulation (Fig. 1A). Among the studied miRNAs, we chose miR-22 and miR-140-3p for further investi-

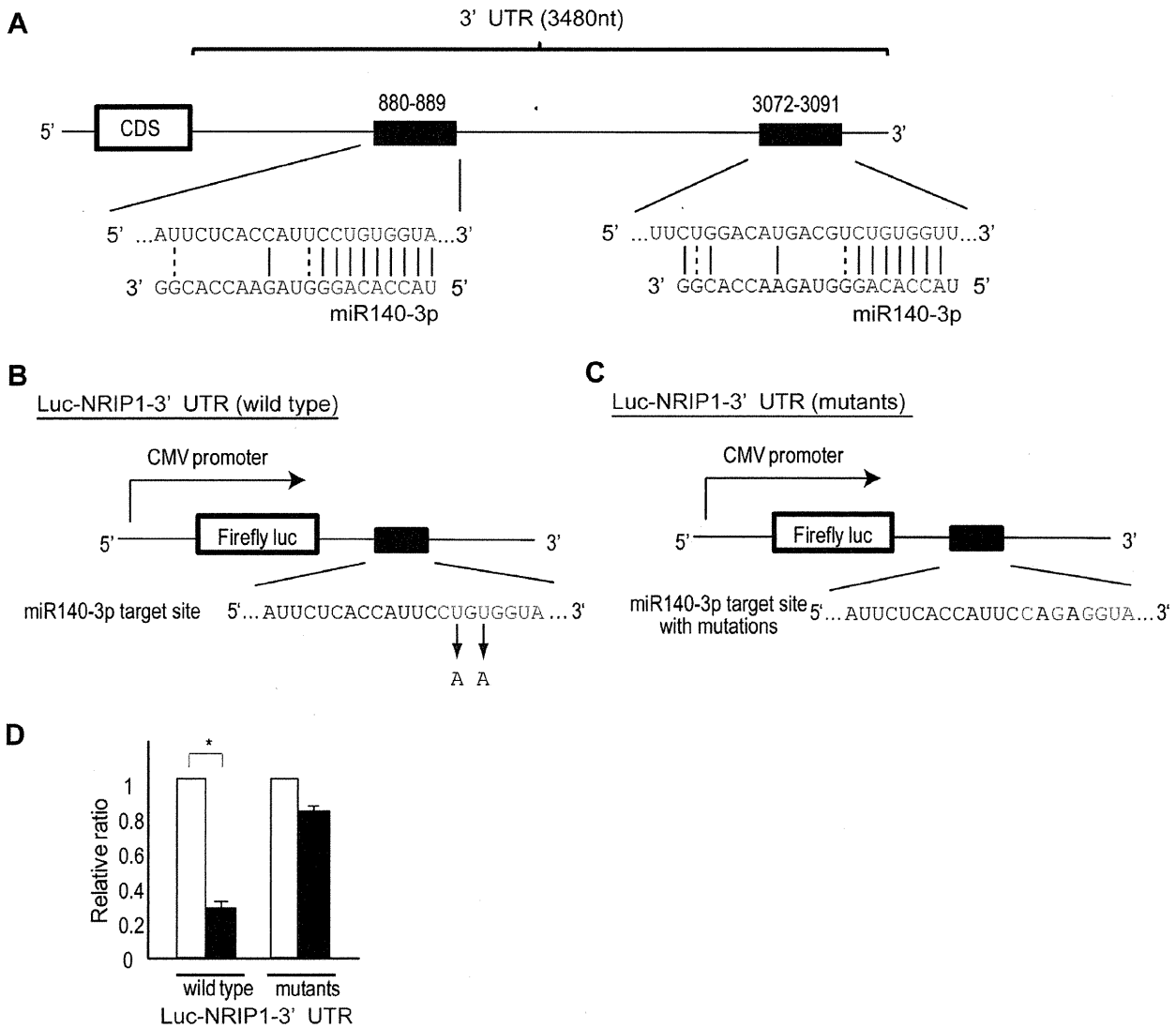

Fig. 3. MiR-140-3p targets the NF-κB coactivator NRIP1. (A) The putative miR-140-3p target sites in the 3′-UTR of human NRIP1. The "seed" sequences of the miR-140-3p-binding sites are shown in red. (B) The luciferase reporter carrying the region of the NRIP1 3′-UTR containing the first putative miR-140-3p target site was used to assess the effects of miR-140-3p on this site. (C) A luciferase reporter with two nucleotide mutations in the "seed sequences" of the putative miR-140-3p target site was constructed. (D) The NRIP1 3′-UTR was directly targeted by miR-140. Huh7 cells were co-transfected with Luc-NRIP1-3′-UTR (wildtype or mutant) and either a control vector (white bar) or an miR-140 precursor-expressing plasmid (black bar) for 24 h, and a luciferase assay was performed. Data represent the mean ± s.d. of three independent experiments.

gation because they suppressed NF-κB activity significantly and reproducibly in two independent screens. We confirmed the effects of transient overexpression of each miRNA using miRNA precursor-expressing plasmids. As predicted, the overexpression of each miRNA precursor significantly suppressed activity of the corresponding reporter containing two nucleotide sequences in the 3′-untranslated region (3′-UTR) complementary to the corresponding miRNA (Supplementary Fig. 1). By transiently transfecting these miRNA precursor-expressing plasmids into HepG2 cells, we showed that miR-22 and miR-140 significantly and reproducibly suppressed TNF-α-stimulated NF-κB reporter activity (Fig. 1B). The effects were NF-κB-specific because no effects were observed for reporters containing point mutations in the NF-κB-binding sites or reporters specific for the transcription factor AP-1 (Supplementary Fig. 2a and b). We also tested miR-122 independently because we had determined that it does not modulate NF-κB activity (Supplementary Fig. S3), but is highly expressed in the liver [17].

2.2. MiR-22 targets the NF-κB coactivator NCOA1

To determine how miR-22 normally regulates NF-κB activity, we searched for potential target genes related to NF-κB using TargetScan (http://www.targetscan.org). Among such potential target genes, NCOA1 (also known as SRC-1) was identified as an NF-κB coactivator [4]. We subsequently showed that luciferase expression from a reporter containing the miR-22 target sites in the 3′-UTR of the NCOA1 mRNA was suppressed by miR-22 precursor overexpression (Fig. 2A and B). Huh7 cells infected with miR-22 precursor-overexpressing lentiviruses exhibited decreased expression of NCOA1 (Fig. 2C), suggesting that NCOA1 expression was regulated by miR-22. In addition, NF-κB activity was inhibited by the knockdown of NCOA1 (Fig. 2D and E). These results suggest that miR-22 enhances NF-κB activity by modulating the expression of the NF-κB coactivator NCOA1.

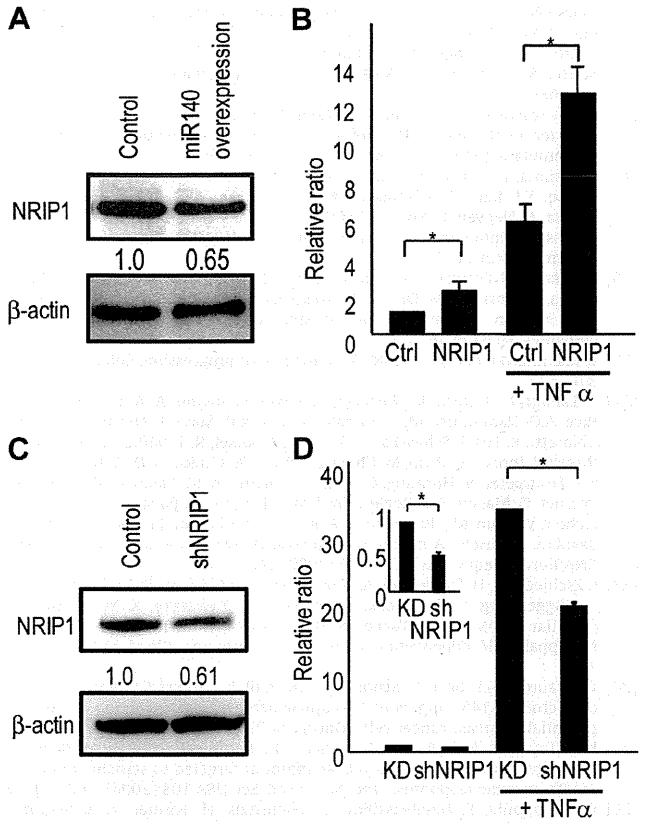

Fig. 4. miR-140-3p regulates NF-κB activity through NRIP1. (A) Overexpression of miR-140 reduces NRIP1 expression. Huh7 cells were infected with miR-140 precursor-expressing lentiviruses, and whole-cell lysates were analyzed by Western blotting using an NRIP1 antibody. Values represent protein levels normalized to the β-actin signal. A result representative of three independent experiments is shown. (B) NRIP1 enhances NF-κB activity. NF-κB activity was measured in TNF-α-stimulated and unstimulated Huh7 cells transiently transfected with an NRIP1-expressing plasmid. $^*p < 0.05$. Data represent the mean ± s.d. of three independent experiments. (C) Confirmation of NRIP1 knockdown in Huh7 cells infected with NRIP1 shRNA-expressing lentiviral particles. (D) Knockdown of NRIP1 reduced NF-κB activation. NF-κB reporter activity was reduced in NRIP1-knockdown Huh7 cells. Data represent the mean ± s.d. of three independent experiments (inset, results from cells not treated with TNF-α). Similar results were obtained using PLC/PRF/5 cells.

2.3. MiR-140-3p targets NRIP1

Similar strategies were applied to characterize the mechanisms by which miR-140-3p regulates NF-κB activity. Among the potential miR-140-3p target genes, we found that the mRNA encoding nuclear receptor-interacting protein 1 (NRIP1, also known as RIP140), a coactivator of NF-κB [23], contains two predicted miR-140-3p target sites in its 3′-UTR (Fig. 3A). We then tested whether miR-140 directly targets NRIP1 by generating a luciferase reporter carrying the region of the NRIP1 3′-UTR that itself contains the first putative miR-140-3p target site (Fig. 3B). To assess specificity, a luciferase construct with two point mutations in the seed sequences of the miR-140-3p target site was also generated (Fig. 3C). Luciferase activity of luc-NRIP1-3′UTR wildtype, but not the mutant reporter construct, was suppressed by overexpression of a miR-140 precursor-expressing plasmid (Fig. 3D), indicating that miR-140-3p directly targets these sequences. In addition, Huh7 cells infected with miR-140 precursor-overexpressing lentiviruses showed decreased expression of NRIP1 (Fig. 4A). These results indicate that NRIP1 is normally targeted by miR-140-3p. We showed that transient overexpression of NRIP1 enhanced NF-κB activity in Huh7 cells (Fig. 4B), consistent with a previous report [23]. In contrast, NF-κB activity was reversed when NRIP1 expression was knocked down (Fig. 4C and D). Therefore, miR-22 and miR-140-3p appear to suppress NF-κB activity through inhibition of distinct NF-κB coactivators [4,23].

3. Discussion

In this study, we have shown that miRNA-22 and miR-140-3p negatively regulate NF-κB by regulating the expression of distinct coactivators—NCOA1 and NRIP1, respectively. The screening method using reporter cell lines and reverse transfection of synthetic miRNAs applied in this study may become a powerful tool in the discovery of miRNAs that modulate intracellular signaling pathways.

Regarding the convergence of miRNAs and NF-κB signaling, several microRNAs have been reported to be involved in NF-κB activation. These include miR-146, miR-155, miR-181b, and miR-21. miR-146 is an NF-κB transcriptional target that itself targets IRAK1 and TRAF6, thereby creating a negative feedback loop [24,25]. miR-155 is highly expressed in a variety of B cell lymphomas and targets IKKs and other genes to create a negative feedback loop [14]. miR-181b is directly regulated by NF-κB and inhibits CYLD expression, which in turn positively regulates NF-κB activity [14,26]. MiR-21, whose expression is increased by NF-κB activation and is elevated in a variety of tumors, is reported to target PTEN and to enhance NF-κB activity [27]. Irrespective of how they regulate NF-κB signaling, most miRNAs that have been reported to be involved in NF-κB signaling are direct targets of NF-κB transactivation and create feedback loops. In this context, it will be interesting to determine whether miR-22 and miR-140-3p, identified in this study as suppressors of NF-κB activity, are also direct NF-κB transactivational genes.

MiR-22 and miR-140-3p target coactivators of NF-κB. To the best of our knowledge, this is the first report on microRNAs that modulate NF-κB activity by regulating the expression of NF-κB coactivators. Because these coactivators may not be NF-κB-specific, it may be important to determine the effects of those miRNAs on other intracellular signaling pathways in which they are possibly involved.

Because NF-κB activation plays a crucial role in human liver tumorigenesis [15,16], and because we identified liver-expressing microRNAs that are important for NF-κB regulation, abnormal reductions in miR-22 and miR140-3p levels in hepatocytes may induce liver carcinogenesis through the enhancement of NF-κB activity. Alternatively, functional impairment of these miRNAs may contribute to hepatocarcinogenesis. Our study provides new information about the involvement of miRNAs in the regulation of NF-κB activity and may help to elucidate the role of NF-κB signaling in pathogenesis in the liver.

Author contributions

A.T. and M.O. conceived the study, planned the research, and wrote the paper. A.T., M.O., K.K., T.Y., and T.K. performed the experiments. H.Y. and K.K. supervised the entire project.

Acknowledgments

This work was supported by Grants-in-Aid from the Ministry of Education, Culture, Sports, Science and Technology, Japan (#22390058 and #80240703) (M.O. and K.Koike), by Health Sciences Research Grants from The Ministry of Health, Labor and Welfare of Japan (Research on Hepatitis) (K.Koike), and by grants from the Mochida Memorial Foundation for Medical and Pharmaceutical Research and from the Araki Memorial Foundation (M.O.).

Appendix A. Supplementary data

Supplementary data associated with this article can be found, in the online version, at doi:10.1016/j.bbrc.2011.07.048.

References

[1] M.S. Hayden, S. Ghosh, Shared principles in NF-kappaB signaling, Cell 132 (2008) 344–362.
[2] M. Karin, Nuclear factor-kappaB in cancer development progression, Nature 441 (2006) 431–436.
[3] G. Bonizzi, M. Karin, The two NF-kappaB activation pathways and their role in innate and adaptive immunity, Trends Immunol. 25 (2004) 280–288.
[4] K.A. Sheppard, D.W. Rose, Z.K. Haque, R. Kurokawa, E. McInerney, S. Westin, D. Thanos, M.G. Rosenfeld, C.K. Glass, T. Collins, Transcriptional activation by NF-kappaB requires multiple coactivators, Mol. Cell. Biol. 19 (1999) 6367–6378.
[5] F. Jin, Y. Li, B. Ren, R. Natarajan, PU.1 C/EBP(alpha) synergistically program distinct response to NF-kappaB activation through establishing monocyte specific enhancers, Proc. Natl. Acad. Sci. USA 108 (2011) 5290–5295.
[6] S.Y. Na, S.K. Lee, S.J. Han, H.S. Choi, S.Y. Im, J.W. Lee, Steroid receptor coactivator-1 interacts with the p50 subunit and coactivates nuclear factor kappaB-mediated transactivations, J. Biol. Chem. 273 (1998) 10831–10834.
[7] R. Lee, R. Feinbaum, V. Ambros, The C. elegans heterochronic gene lin-4 encodes small RNAs with antisense complementarity to lin-14, Cell 75 (1993) 843–854.
[8] J. Carrington, V. Ambros, Role of microRNAs in plant and animal development, Science 301 (2003) 336–338.
[9] D. Bartel, MicroRNAs: genomics, biogenesis, mechanism, and function, Cell 116 (2004) 281–297.
[10] V. Ambros, The functions of animal microRNAs, Nature 431 (2004) 350–355.
[11] J. Lu, G. Getz, E. Miska, E. Alvarez-Saavedra, J. Lamb, D. Peck, A. Sweet-Cordero, B. Ebert, R. Mak, A. Ferrando, J. Downing, T. Jacks, H. Horvitz, T. Golub, MicroRNA expression profiles classify human cancers, Nature 435 (2005) 834–838.
[12] S.Y. Park, J.H. Lee, M. Ha, J.W. Nam, V.N. Kim, MiR-29 miRNAs activate p53 by targeting p85 alpha and CDC42, Nat. Struct. Mol. Biol. 16 (2009) 23–29.
[13] A.L. Kasinski, F.J. Slack, Potential microRNA therapies targeting Ras, NFkappaB and p53 signaling, Curr. Opin. Mol. Ther. 12 (2010) 147–157.
[14] X. Ma, L.E. Becker Buscaglia, J.R. Barker, Y. Li, MicroRNAs in NF-{kappa}B signaling, J. Mol. Cell. Biol. 3 (2011) 159–166.
[15] T. Block, A. Mehta, C. Fimmel, R. Jordan, Molecular viral oncology of hepatocellular carcinoma, Oncogene 22 (2003) 5093–5107.
[16] J. Ji, J. Shi, A. Budhu, Z. Yu, M. Forgues, S. Roessler, S. Ambs, Y. Chen, P. Meltzer, C. Croce, L. Qin, K. Man, C. Lo, J. Lee, I. Ng, J. Fan, Z. Tang, H. Sun, X. Wang, MicroRNA expression, survival, and response to interferon in liver cancer, N. Engl. J. Med. 361 (2009) 1437–1447.
[17] J. Krützfeldt, N. Rajewsky, R. Braich, K. Rajeev, T. Tuschl, M. Manoharan, M. Stoffel, Silencing of microRNAs in vivo with 'antagomirs', Nature 438 (2005) 685–689.
[18] J. Miyagawa, M. Muguruma, H. Aoto, I. Suetake, M. Nakamura, S. Tajima, Isolation of the novel cDNA of a gene of which expression is induced by a demethylating stimulus, Gene 240 (1999) 289–295.
[19] K. Kojima, A. Takata, C. Vadnais, M. Otsuka, T. Yoshikawa, M. Akanuma, Y. Kondo, Y.J. Kang, T. Kishikawa, N. Kato, Z. Xie, W.J. Zhang, H. Yoshida, M. Omata, A. Nepveu, K. Koike, MicroRNA122 is a key regulator of α-fetoprotein, expression influences the aggressiveness of hepatocellular carcinoma, Nat. Commun. 2 (2011) 338.
[20] A. Takata, M. Otsuka, T. Kogiso, K. Kojima, T. Yoshikawa, R. Tateishi, N. Kato, S. Shiina, H. Yoshida, M. Omata, K. Koike, Direct differentiation of hepatic cells from human induced pluripotent stem cells using a limited number of cytokines, Hepatol. Int. (2011).
[21] L. Ma, R.A. Weinberg, MicroRNAs in malignant progression, Cell Cycle 7 (2008) 570–572.
[22] P. Landgraf, M. Rusu, R. Sheridan, A. Sewer, N. Iovino, A. Aravin, S. Pfeffer, A. Rice, A.O. Kamphorst, M. Landthaler, C. Lin, N.D. Socci, L. Hermida, V. Fulci, S. Chiaretti, R. Foà, J. Schliwka, U. Fuchs, A. Novosel, R.U. Müller, B. Schermer, U. Bissels, J. Inman, Q. Phan, M. Chien, D.B. Weir, R. Choksi, G. De Vita, D. Frezzetti, H.I. Trompeter, V. Hornung, G. Teng, G. Hartmann, M. Palkovits, R. Di Lauro, P. Wernet, G. Macino, C.E. Rogler, J.W. Nagle, J. Ju, F.N. Papavasiliou, T. Benzing, P. Lichter, W. Tam, M.J. Brownstein, A. Bosio, A. Borkhardt, J.J. Russo, C. Sander, M. Zavolan, T. Tuschl, A mammalian microRNA expression atlas based on small RNA library sequencing, Cell 129 (2007) 1401–1414.
[23] I. Zschiedrich, U. Hardeland, A. Krones-Herzig, M. Berriel Diaz, A. Vegiopoulos, J. Müggenburg, D. Sombroek, T. Hofmann, R. Zawatzky, X. Yu, N. Gretz, M. Christian, R. White, M. Parker, S. Herzig, Coactivator function of RIP140 for NFkappaB/RelA-dependent cytokine gene expression, Blood 112 (2008) 264–276.
[24] D. Bhaumik, G.K. Scott, S. Schokrpur, C.K. Patil, J. Campisi, C.C. Benz, Expression of microRNA-146 suppresses NF-kappaB activity with reduction of metastatic potential in breast cancer cells, Oncogene 27 (2008) 5643–5647.
[25] K.D. Taganov, M.P. Boldin, K.J. Chang, D. Baltimore, NF-kappaB-dependent induction of microRNA, miR-146, an inhibitor targeted to signaling proteins of innate immune responses, Proc. Natl. Acad. Sci. USA 103 (2006) 12481–12486.
[26] E. Trompouki, E. Hatzivassiliou, T. Tsichritzis, H. Farmer, A. Ashworth, G. Mosialos, CYLD is a deubiquitinating enzyme that negatively regulates NF-kappaB activation by TNFR family members, Nature 424 (2003) 793–796.
[27] D. Iliopoulos, S.A. Jaeger, H.A. Hirsch, M.L. Bulyk, K. Struhl, STAT3 activation of miR-21 and miR-181b-1 via and PTEN and CYLD are part of the epigenetic switch linking inflammation to cancer, Mol. Cell. 39 (2010) 493–506.

Living Donor Liver Transplantations in HIV- and Hepatitis C Virus-Coinfected Hemophiliacs: Experience in a Single Center

Kunihisa Tsukada,[1,2] Yasuhiko Sugawara,[3,10] Junichi Kaneko,[3] Sumihito Tamura,[3] Natsuo Tachikawa,[2,4] Yuji Morisawa,[1,5] Shu Okugawa,[1] Yoshimi Kikuchi,[2] Shinichi Oka,[2] Satoshi Kimura,[1,2,6] Yutaka Yatomi,[7] Masatoshi Makuuchi,[8] Norihiro Kokudo,[3] and Kazuhiko Koike[1,9]

Background. Although almost all human immunodeficiency virus (HIV)-infected Japanese hemophiliacs are coinfected with hepatitis C virus (HCV), the outcome of living donor liver transplantation (LDLT) in such patients in terms of survival rate, perioperative complications, and recovery of coagulation activity is poorly understood.
Patients and Methods. Six HIV-positive hemophiliacs underwent LDLT for HCV-associated advanced cirrhosis. The mean CD4 T-cell count at transplantation was 376±227/μL.
Results. The 1-, 3-, and 5-year survival rates were 66%, 66%, and 50%, respectively. Fatal perioperative bleeding related to hemophilia was not observed. Two patients died within 6 months after transplantation due to graft failure. HIV infection was well controlled in all patients who survived longer than 6 months. Two patients (genotype 2a and 2+3a) achieved a sustained viral response and both of them were alive at the end of follow-up period, whereas one patient (genotype 1a+1b) died of decompensated cirrhosis 4 years after transplantation due to recurrent HCV infection.
Conclusions. HIV/HCV-coinfected hemophiliacs can safely undergo LDLT. Hemophilia was clinically cured after successful transplantation. A good outcome can be expected as long as postoperative hepatitis C is controlled with interferon/ribavirin combination therapy.

Keywords: Hepatitis C virus, Living donor liver transplantation, HIV, HAART.

(*Transplantation* 2011;91: 1261–1264)

Because of the availability of highly active antiretroviral therapy (HAART), the life expectancy of patients infected with human immunodeficiency virus (HIV) has dramatically improved (*1*). Death from opportunistic infections has decreased and, as the result, non-acquired immune deficiency syndrome (AIDS)-defining complications such as hepatic diseases, cardiovascular diseases, or non-AIDS malignancies have emerged as the most important problems (*2*, *3*).

Hepatitis C virus (HCV) and HIV often coinfect due to their shared route of transmission. A recent report indicated that approximately 20% of HIV-infected people in Japan are coinfected with HCV (*4*), a large proportion of whom are hemophiliacs. Approximately 1500 hemophiliacs were infected with HIV through non heat-treated concentrated coagulation factor administration between 1981 and 1985, and 98% of them were also infected with HCV. The coexistence of HIV infection with HCV accelerates the progression of liver fibrosis (*5*) and attenuates the efficacy of interferon (IFN) treatment for HCV (*6*, *7*). A considerable number of such coinfected patients suffer from decompensated cirrhosis or hepatocellular carcinoma (HCC) (*8*). In the HAART era, AIDS-related death is gradually decreasing (*9*) and HCV-

This work was supported by a Grant-in-aid for Scientific Research from the Ministry of Education, Culture, Sports, Science and Technology of Japan and from the Ministry of Health, Labor and Welfare of Japan (AIDS Research).

[1] Department of Infectious Diseases, Graduate School of Medicine, the University of Tokyo, Bunkyo-Ku, Tokyo.
[2] AIDS Clinical Center, National Center for Global Health and Medicine, Shinjuku-ku, Tokyo, Japan.
[3] Division of Artificial Organ and Transplantation, Department of Surgery, the University of Tokyo, Bunkyo-Ku, Tokyo.
[4] Yokohama Municipal Citizens Hospital, Yokohama, Japan.
[5] Department of Infection Control, Jichi Medical School, Tochigi-ken, Japan.
[6] Tokyo Teishin Hopital, Chiyoda-ku, Tokyo, Japan.
[7] Department of Clinical Laboratory Medicine, the University of Tokyo, Bunkyo-Ku, Tokyo.
[8] Japanese Red Cross Hospital, Shibuya-Ku, Tokyo, Japan.
[9] Department of Gastroenterology, Graduate School of Medicine, the University of Tokyo, Bunkyo-Ku, Tokyo.
[10] Address correspondence to: Yasuhiko Sugawara, M.D., Division of Artificial Organ and Transplantation, Department ofSurgery, University of Tokyo, 7-3-1 Hongo, Bunkyo-Ku, Tokyo.
E-mail: yasusugatky@yahoo.co.jp

K.T., Y.S., J.K., S.T., Y.Y., M.M., N.K., and K.K. participated in research design; K.T. and Y.S. participated in the writing of the manuscript; and N.T., Y.M., S.O., Y.K., S.O., and S.K. participated in the performance of the research.
Received 2 December 2010. Revision requested 3 January 2011.
Accepted 7 March 2011.

ISSN 0041-1337/11/9111-1261
DOI: 10.1097/TP.0b013e3182193cf3

related liver diseases have become the leading cause of death in Japanese hemophiliacs (*10*).

The only curative treatment for end-stage liver disease is liver transplantation. In the pre-HAART era, HIV infection was considered an absolute or relative contraindication for transplantation. Several cases were reported during that period (*11*, *12*), but the outcomes were not always satisfactory. In the HAART era, more than 50 cases of HIV-positive liver transplantation have been reported (*13–21*), and survival after liver transplantation seems to be more promising.

The absolute number of deceased donor livers in Japan is small, and living donor liver transplantation (LDLT) is the mainstay of liver transplantation. We reported the first LDLT in an HIV-positive hemophiliac in 2002 (*22*). Here, we present a series of six cases of LDLT in HIV/HCV-coinfected hemophiliacs performed at the University of Tokyo Hospital between 2001 and 2004.

RESULTS

Survival

The 1-, 3-, and 5-year survival rates were 66%, 66%, and 50%, respectively. Two patients (cases 2 and 5) died on postoperative day (POD) 99 and 156, respectively. The causes of early death were graft failure and bleeding from cytomegalovirus (CMV) enteritis (case 2) and graft failure suspected to be cholestatic hepatitis (case 5). One patient died 50 months after LDLT due to recurrent HCV-related cirrhosis.

Results of Antiviral Therapy for Recurrent Hepatitis C in the Graft

After LDLT, all but one (case 2) patients received combination therapy with IFN (standard or pegylated form) and ribavirin. Case 3 was treated for biopsy-proven recurrent hepatitis C, whereas the other four were treated preemptively (started on POD, 10–70 days). Duration of anti-HCV therapy was 12 months in case early viral response was achieved. Cases 1 and 3 achieved sustained viral response (SVR). Case 3 suffered from HCV-related cholestatic hepatitis on POD 38, which responded well to combination therapy with IFN and ribavirin and he eventually achieved SVR. The other patients did not achieve SVR. Cases 4 and 6 showed a biochemical response and were on maintenance antiviral therapy. In case 6, tacrolimus was switched to cyclosporine A 15 months after LDLT to suppress HCV replication. This lead to a transient 10-fold decrease in HCV-RNA, but it returned to the previous value within several months.

Results of Antiretroviral Therapy After LDLT

Antiretroviral therapy was transiently terminated during the perioperative period. The timing of reintroduction was individualized according to the CD4 count, HIV viral load, general status such as surgical complication and the result of liver function tests. One patient (case 1) has continued to maintain a high CD4 count without antiretroviral therapy. One patient (case 2) died before antiretroviral reintroduction.

The remaining four patients started antiretroviral therapy at a median of 56.5 days after LDLT (range, 43–485 days). The choice of the antiretroviral drug was individualized according to each patient's antiretroviral history and accumulated resistance mutations. A protease inhibitor-based combination was selected in all cases. All but one patient (case 5) tolerated antiretroviral therapy and had an excellent response. The blood concentration of the immunosuppressant increased drastically from the first day of protease inhibitor administration, which was controlled by close monitoring and dosage modification.

Elevation of serum alkaline-phosphatase and gamma-glutanyl-transpeptidase values was observed in all patients after antiretroviral reintroduction. Other significant adverse effects include severe allergic reaction to lamivudine (case 3) and liver failure, which was clinically diagnosed to be cholestatic hepatitis as an immune reconstitution inflammatory syndrome against HCV (case 5).

One patient (case 3) developed Burkitt leukemia 38 months after LDLT. His CD4 count at that time was 480/μL and HIV-RNA was undetectable. Combination chemotherapy using cyclophosphamide, vincristine, doxorubicin, and dexamethasone (*23*) was effective, and he eventually achieved complete remission. Other opportunistic infections included multiple abscess formation at the surgical site in two patients (case 2 by methicillin-resistant *Staphylococcus aureus* and case 5 by multi-drug resistant *Pseudomonas aeruginosa*). Positive CMV antigenemia was observed in all cases. However, only one patient (case 2) presented with clinically overt organ damage.

Restoration of Coagulation After LDLT

Except for case 5, replacement became unnecessary within 1 week after operation. In case 5, in addition to insufficient endogenous coagulation factor production, re-operation was necessary several times, and the coagulation factor replacement could not be withdrawn. Cases 2 and 6 again required coagulation factor replacement after graft failure became apparent.

Outcome of the Donors

All donors were alive without major complications at the point of analysis. Two donors were considered obligate carriers of hemophilia and one of them (donor of case 5) showed relatively low coagulation activity, but none of the donors experienced abnormal bleeding requiring coagulation factor administration. The donor of case 5 experienced transient decrease in factor IX activity after liver resection. However, the value of coagulation activity recovered without supplementation.

DISCUSSION

Recurrence of hepatitis C is the most important problem in treating HCV-positive hemophiliac patients. Recent reports indicate that HIV/HCV-coinfected liver recipients have a relatively lower survival rate than HCV-monoinfected liver recipients, although the difference is not significant. In our series, two of three deaths were related to recurrent HCV, and two patients experienced fibrosing cholestatic hepatitis. Cholestatic hepatitis is characterized by a high rate of HCV replication and a paucity of inflammatory activity, and the risk might increase in LDLT recipients (*24*, *25*). In our center, IFN therapy is usually introduced preemptively as soon as possible. In our series, two cases infected with non-1b virus achieved SVR, whereas others did not achieve SVR. A report demonstrated the effectiveness of maintenance therapy with

pegylated (PEG)-IFN plus ribavirin (*26*), but this efficacy was not apparent in our series. Combination antiviral therapy with protease and polymerase inhibitors may improve the treatment results in the future.

With regard to HIV infection, when to restart antiretroviral therapy after LDLT has remained a question. Hemophiliacs often have a long-term treatment history. Five of six cases had a multiple history of treatment failure, and as a result, only one or two reliable antiretroviral combinations were available to each patient in that era. Protease inhibitors, key drugs for successful HIV suppression in such cases have a potential risk of liver toxicity, especially in those with HCV coinfection (*27*). Unlike whole liver transplantation, the initial graft size is relatively small in LDLT. The graft gradually increases its volume within several weeks after transplantation, and an unfavorable effect of antiretroviral treatment on graft growth during this period is a concern. Moreover, unintended treatment interruption due to early phase complications may result in further accumulation of resistance-associated mutations. Taking these issues into account, we delayed starting antiretroviral therapy until at least 4 weeks after LDLT. It is obvious, however, that earlier antiretroviral reintroduction has more benefit toward reducing opportunistic infections and improving the result of anti-HCV therapy after LDLT. The effectiveness and safety of a new class antiretrovirals, raltegravir (*28*), and enfuvirtide (*29*), were recently reported, and these compounds may play an important role in the management of HIV-infected split-graft recipients.

In our series, the immunosuppressant trough level was targeted to the same level as that in HIV-negative cases. It is not known, however, whether HIV-infected patients, particularly those with a relatively lower CD4 cell count, need the same blood level of immunosuppressants. Moreover, the CD4 cell count, may not act as accurate surrogate marker for immune function in those taking an immunosuppressant or steroid. In case 2, recurrent bleeding from CMV intestinal ulcer eventually led to death after immunosuppression was intensified to treat severe graft rejection. In this case, antiretroviral therapy could not be reintroduced because of severe liver damage, which might enhance excess immunosuppression. A more precise indicator than CD4 count and immunosuppressant level is needed. Dose modification of immunosuppressive drugs using an immune function assay (*30*) may contribute to more precise management, especially in HIV-coinfected patients.

A considerable number of HIV/HCV-coinfected patients are suffering from decompensated cirrhosis or HCC (*8*), and some of them are potential candidates for future liver transplantation. The shortage of deceased donor liver grafts is a major problem worldwide. LDLT can overcome such a problem. Clearly, regenerative medicine will have an important role in this field in the future. Those patients who are already in a cirrhotic state, however, cannot wait for such an innovative modality to be established. In our series, all patients who tolerated antiretroviral therapy achieved good HIV control, and those who cleared HCV survived long. Clinical cure of hemophilia after successful transplantation drastically improved the patients' quality of life. Cure of hemophilia also lead to considerable cost reduction. LDLT continues to have an important role in HIV-infected hemophiliacs.

MATERIALS AND METHODS

From April 2001 to October 2004, nine HIV/HCV-coinfected patients were referred to the University of Tokyo hospital for LDLT. The indication was HCV-related end-stage liver disease.

HIV-positive patients should meet the same standard criteria for liver transplantation as HIV-negative patients. The criteria for accepting candidates for LDLT were absolute CD4 T lymphocyte count more than 200/μL, or more than 14% CD4 proportion to total lymphocytes when hypersplenism-related leukocytopenia was considered the cause of an apparent decrease in the CD4 count. Undetectable HIV RNA was not required as long as effective HIV suppression was expected after transplantation. Exclusion criteria related to HIV infection were active AIDS-defining diseases except for esophageal candidiasis. All cases were approved by the ethics committee at the University of Tokyo. Donor was selected from those with spontaneous will and within the third-degree consanguinity of the patient. Those with abnormal coagulation values were excluded from candidate for the donor.

Two patients did not meet the criteria (one with concomitant uncontrollable fungal infection and one without appropriate donor). One patient retracted consent before operation. Finally, six HIV/HCV-coinfected hemophiliacs underwent LDLT. Two patients were transplanted emergently (within 2 weeks after referral) because of progressive hepatic encephalopathy and hepatorenal syndrome. None of the patients had concomitant active hepatitis B, HCC, or other malignancies. The patient characteristics are summarized in Table 1.

The appropriate type of concentrated coagulation factor was administered during the perioperative period. Concentrated coagulation factor was administered as a bolus just before the operation to achieve 100% coagulating

TABLE 1. Patient characteristics at LDLT and outcome

Case	Age/ sex	Type of hemophilia	HCV genotype	HCV-RNA at LDLT (KIU/mL)	HIV load (copy/mL)	MELD at LDLT	CCr	HTN/ DM	BMI	Graft	Graft size (%SLV)	ACR	CMV	Survival (mo)	Donor
1	41M	B	2a	3	UD	23	24	N/N	19.1	Right	66	0	1	Alive (115)	Brother
2	28M	A	2a, 2b	1410	6.2×10^4	15	76	N/N	23.4	Right	57	2	2	Died (3)	Mother
3	30M	A	1b, 3a	740	3.2×10^4	15	78	N/N	21.5	Right	42	1	2	Alive (96)	Mother
4	38M	A	1b, 3a	200	UD	34	69	N/N	20.0	Right	47	1	1	Alive (82)	Sister
5	31M	B	1a	747	2.6×10^4	18	72	N/N	24.3	Right	47	2	3	Died (5)	Mother
6	32M	B	1a, 1b	41	UD	48	62	N/N	25.2	Right	63	0	0	Died (50)	Father

HCV, hepatitis C virus; LDLT, living donor liver transplantation; HIV, human immunodeficiency virus; MELD, model for end-stage liver disease; CCr, creatine clearance; HTN, hypertension; DM, diabetes mellitus; BMI, body mass index; SLV, standard liver volume; ACR, acute cellular rejection; CMV, cytomegalovirus; UD, undetectable.

factor activity, followed by continuous infusion to maintain greater than 80% activity during the operation. Fresh-frozen plasma was also replaced. Initial dosage of the coagulation factor was calculated based on the results of preoperative pharmacokinetic studies, and the rate of continuous infusion was adjusted as necessary by periodical monitoring of coagulation factor activity.

Tacrolimus and steroids based immunosuppression was planned as previously described (*31*). The target tacrolimus trough level was same as that for the HIV-negative population. Moderate to severe rejection was treated with pulse steroids±mycophenolate mofetil.

The preoperative HCV-RNA value was positive in all subjects. The HCV genotype is listed in Table 1. All patients underwent concomitant splenectomy (*32*). Preemptive anti-HCV therapy with IFN (standard or pegylated form) plus ribavirin was planned after LDLT (*33*). Postoperative CMV reactivation was monitored using a pp65 antigen detecting method (CMV antigenemia), and a positive result was preemptively treated with ganciclovir (*34*) or valganciclovir.

ACKNOWLEDGMENTS

The authors thank Dr. Fukutake, Department of Laboratory Medicine, Tokyo Medical School, and Drs. Kusama and Nakajima at the Pharmaceutical Department in the University of Tokyo Hospital for technical support of perioperative coagulation management.

REFERENCES

1. Mocroft A, Ledergerber B, Katlama C, et al. Decline in the AIDS and death rates in the EuroSIDA study: An observational study. *Lancet* 2003; 362: 22.
2. Palella FJ Jr, Baker RK, Moorman AC, et al. Mortality in the highly active antiretroviral therapy era: Changing causes of death and disease in the HIV outpatient study. *J Acquir Immune Defic Syndr* 2006; 43: 27.
3. Weber R, Sabin CA, Friis-Moller N, et al. Liver-related deaths in persons infected with the human immunodeficiency virus: The D:A:D study. *Arch Intern Med* 2006; 166: 1632.
4. Koike K, Tsukada K, Yotsuyanagi H, et al. Prevalence of coinfection with human immunodeficiency virus and hepatitis C virus in Japan. *Hepatol Res* 2007; 37: 2.
5. Mohsen AH, Easterbrook PJ, Taylor C, et al. Impact of human immunodeficiency virus (HIV) infection on the progression of liver fibrosis in hepatitis C virus infected patients. *Gut* 2003; 52: 1035.
6. Chung RT, Andersen J, Volberding P, et al. Peginterferon alfa-2a plus ribavirin versus interferon alfa-2a plus ribavirin for chronic hepatitis C in HIV-coinfected persons. *N Engl J Med* 2004; 351: 451.
7. Torriani FJ, Rodriguez-Torres M, Rockstroh JK, et al. Peginterferon Alfa-2a plus ribavirin for chronic hepatitis C virus infection in HIV-infected patients. *N Engl J Med* 2004; 351: 438.
8. Yotsuyanagi H, Kikuchi Y, Tsukada K, et al. Chronic hepatitis C in patients co-infected with human immunodeficiency virus in Japan: A retrospective multicenter analysis. *Hepatol Res* 2009; 39: 657.
9. Tatsunami S, Fukutake K, Taki M, et al. Observed decline in the rate of death among Japanese hemophiliacs infected with HIV-1. *Int J Hematol* 2000; 72: 256.
10. Tatsunami S, Taki M, Shirahata A, et al. Increasing incidence of critical liver disease among causes of death in Japanese hemophiliacs with HIV-1. *Acta Haematol* 2004; 111: 181.
11. Tzakis AG, Cooper MH, Dummer JS, et al. Transplantation in HIV+ patients. *Transplantation* 1990; 49: 354.
12. Gordon FH, Mistry PK, Sabin CA, et al. Outcome of orthotopic liver transplantation in patients with haemophilia. *Gut* 1998; 42: 744.
13. Moreno-Cuerda VJ, Morales-Conejo M. Liver transplantation in patients with HIV infection. *Gastroenterol Hepatol* 2005; 28: 258.
14. Neff GW, Bonham A, Tzakis AG, et al. Orthotopic liver transplantation in patients with human immunodeficiency virus and end-stage liver disease. *Liver Transpl* 2003; 9: 239.
15. Norris S, Taylor C, Muiesan P, et al. Outcomes of liver transplantation in HIV-infected individuals: The impact of HCV and HBV infection. *Liver Transpl* 2004; 10: 1271.
16. Fung J, Eghtesad B, Patel-Tom K, et al. Liver transplantation in patients with HIV infection. *Liver Transpl* 2004; 10: S39.
17. Vogel M, Voigt E, Schafer N, et al. Orthotopic liver transplantation in human immunodeficiency virus (HIV)-positive patients: Outcome of 7 patients from the Bonn cohort. *Liver Transpl* 2005; 11: 1515.
18. Roland ME, Stock PG. Liver transplantation in HIV-infected recipients. *Semin Liver Dis* 2006; 26: 273.
19. Mindikoglu AL, Regev A, Magder LS. Impact of human immunodeficiency virus on survival after liver transplantation: Analysis of United Network for Organ Sharing database. *Transplantation* 2008; 85: 359.
20. Tateo M, Roque-Afonso AM, Antonini TM, et al. Long-term follow-up of liver transplanted HIV/hepatitis B virus coinfected patients: Perfect control of hepatitis B virus replication and absence of mitochondrial toxicity. *AIDS* 2009; 23: 1069.
21. Testillano M, Fernandez JR, Suarez MJ, et al. Survival and hepatitis C virus recurrence after liver transplantation in HIV- and hepatitis C virus-coinfected patients: Experience in a single center. *Transplant Proc* 2009; 41: 1041.
22. Sugawara Y, Ohkubo T, Makuuchi M, et al. Living-donor liver transplantation in an HIV-positive patient with hemophilia. *Transplantation* 2002; 74: 1655.
23. Cortes J, Thomas D, Rios A, et al. Hyperfractionated cyclophosphamide, vincristine, doxorubicin, and dexamethasone and highly active antiretroviral therapy for patients with acquired immunodeficiency syndrome-related Burkitt lymphoma/leukemia. *Cancer* 2002; 94: 1492.
24. Troppmann C, Rossaro L, Perez RV, et al. Early, rapidly progressive cholestatic hepatitis C reinfection and graft loss after adult living donor liver transplantation. *Am J Transplant* 2003; 3: 239.
25. Gaglio PJ, Malireddy S, Levitt BS, et al. Increased risk of cholestatic hepatitis C in recipients of grafts from living versus cadaveric liver donors. *Liver Transpl* 2003; 9: 1028.
26. Kornberg A, Kupper B, Tannapfel A, et al. Antiviral maintenance treatment with interferon and ribavirin for recurrent hepatitis C after liver transplantation: Pilot study. *J Gastroenterol Hepatol* 2007; 22: 2135.
27. Sulkowski MS. Drug-induced liver injury associated with antiretroviral therapy that includes HIV-1 protease inhibitors. *Clin Infect Dis* 2004; 38: S90.
28. Tricot L, Teicher E, Peytavin G, et al. Safety and efficacy of raltegravir in HIV-infected transplant patients cotreated with immunosuppressive drugs. *Am J Transplant* 2009; 9: 1946.
29. Teicher E, Abbara C, Duclos-Vallee JC, et al. Enfuvirtide: A safe and effective antiretroviral agent for human immunodeficiency virus-infected patients shortly after liver transplantation. *Liver Transpl* 2009; 15: 133.
30. Kowalski RJ, Post DR, Mannon RB, et al. Assessing relative risks of infection and rejection: A meta-analysis using an immune function assay. *Transplantation* 2006; 82: 663.
31. Sugawara Y, Makuuchi M, Kaneko J, et al. Correlation between optimal tacrolimus doses and the graft weight in living donor liver transplantation. *Clin Transplant* 2002; 16: 102.
32. Kishi Y, Sugawara Y, Akamatsu N, et al. Splenectomy and preemptive interferon therapy for hepatitis C patients after living-donor liver transplantation. *Clin Transplant* 2005; 19: 769.
33. Sugawara Y, Makuuchi M, Matsui Y, et al. Preemptive therapy for hepatitis C virus after living-donor liver transplantation. *Transplantation* 2004; 78: 1308.
34. Koetz AC, Delbruck R, Furtwangler A, et al. Cytomegalovirus pp65 antigen-guided preemptive therapy with ganciclovir in solid organ transplant recipients: A prospective, double-blind, placebo-controlled study. *Transplantation* 2001; 72: 1325.

Original Article

Hepatocellular Carcinoma With Extrahepatic Metastasis

Clinical Features and Prognostic Factors

Koji Uchino, MD[1]; Ryosuke Tateishi, MD, PhD[1]; Shuichiro Shiina, MD, PhD[1]; Miho Kanda, MD, PhD[2]; Ryota Masuzaki, MD, PhD[1]; Yuji Kondo, MD, PhD[1]; Tadashi Goto, MD, PhD[1]; Masao Omata, MD, PhD[3]; Haruhiko Yoshida, MD, PhD[1]; and Kazuhiko Koike, MD, PhD[1]

BACKGROUND: Despite significant advances in the treatment of intrahepatic lesions, the prognosis for patients with hepatocellular carcinoma (HCC) who have extrahepatic metastasis remains poor. The objective of this study was to further elucidate the clinical course and prognostic determinants of patients with this disease. **METHODS:** In total, 342 patients who had HCC with extrahepatic metastasis were enrolled. The metastases were diagnosed at initial presentation with HCC in 28 patients and during follow-up in the remaining patients. The authors analyzed clinical features, prognoses, and treatments and established a scoring system to predict prognosis using a split-sample method with a testing set and a training set. **RESULTS:** The most frequent site of extrahepatic metastasis was the lung followed by lymph nodes, bone, and adrenal glands. These metastases were related directly to death in only 23 patients (7.6%). The median survival after diagnosis of extrahepatic metastasis was 8.1 months (range, 0.03-108.7 months). In univariate analysis of the training set (n = 171), performance status, Child-Pugh classification, the number and size of intrahepatic lesions, macroscopic vascular invasion, symptomatic extrahepatic metastases, α-fetoprotein levels, and complete responses to treatment were associated significantly with prognosis. On the basis of multivariate analysis, a scoring system was developed to predict prognosis that assessed uncontrollable intrahepatic lesions, extent of vascular invasion, and performance status. This scoring system was validated in the testing set (n = 171) and produced a concordance index of 0.73. **CONCLUSIONS:** The controllability of intrahepatic lesions and performance status were identified as important prognostic factors in patients with advanced HCC who had extrahepatic metastasis. *Cancer* **2011;117:4475-83.** © *2011 American Cancer Society.*

KEYWORDS: hepatocellular carcinoma, extrahepatic metastasis, clinical course, prognosis.

Hepatocellular carcinoma (HCC) is a leading cause of cancer death, and its incidence is particularly high in Asian countries, including Japan.[1,2] HCC usually develops in a liver that already suffers from chronic disease, most notably because of hepatitis B virus (HBV) or hepatitis C virus (HCV) infection.[3] In the past, HCC often was diagnosed only at a far advanced stage, and this was accompanied by a very poor prognosis.[4] However, today, close surveillance with advanced diagnostic modalities on designated high-risk patients has facilitated the detection of HCC at a much early stage. Together with the considerable advances in treatment for HCC, such as surgical resection, percutaneous ablation, transcatheter arterial chemoembolization (TACE), and liver transplantation, the survival of HCC patients has improved much in recent years.[5-9]

Primary HCC lesions often can be removed completely when they are detected at an early stage. Although intrahepatic recurrence of HCC is very frequent, recurrent intrahepatic lesions can be treated successfully using modalities applicable to primary lesions. In particular, percutaneous ablation can be performed repeatedly on recurrent intrahepatic lesions even in patients with moderately impaired liver function. Thus, intrahepatic lesions can be kept under control, but extrahepatic metastasis still may arise.[10,11] Extrahepatic metastasis of HCC were once regarded as a terminal event,[12] and coexisting intrahepatic lesions usually are not treated by locoregional therapies like surgical resection or medical ablation.[13] Although systemic chemotherapies sometimes have been attempted, no standard protocols were established until

Corresponding author: Haruhiko Yoshida, MD, PhD, Department of Gastroenterology, Graduate School of Medicine, The University of Tokyo, 7-3-1 Hongo, Bunkyo-ku, Tokyo 113-8655, Japan; Fax: (011) 81-3-3814-0021; yoshida-2im@h.u-tokyo.ac.jp

[1]Department of Gastroenterology, Graduate School of Medicine, The University of Tokyo, Tokyo, Japan; [2]Department of Gastroenterology and Hepatology, Kyoundo Hospital, Tokyo, Japan; [3]Yamanashi Prefectural Hospital Organization, Yamanashi, Japan

DOI: 10.1002/cncr.25960, **Received:** September 4, 2010; **Revised:** December 27, 2010; **Accepted:** January 3, 2011, **Published online** March 22, 2011 in Wiley Online Library (wileyonlinelibrary.com)

recently.[14,15] In 2 recent, large, randomized controlled trials, it was demonstrated that the multikinase inhibitor sorafenib significantly prolonged survival in patients with advanced HCC, even when the primary lesion was accompanied by extrahepatic metastases; now, sorafenib is widely regarded as the standard treatment for such patients.[16,17] However, the clinical course for patients with extrahepatic metastasis has not yet been fully elucidated, and the prognostic factors remain unclear. This information will be vital when determining whether treatment with sorafenib or other such agents is indicated.

The prognosis for patients with HCC who had extrahepatic metastasis before the availability of sorafenib may represent the natural clinical course for affected patients, because no previous treatments had proven effective. In the current study, we retrospectively analyzed a cohort of these patients to further investigate the clinical features and prognostic factors for HCC with extrahepatic metastasis.

MATERIALS AND METHODS

Patients

This study was conducted according to the ethical guidelines for epidemiologic research designed by the Ministry of Education, Culture, Sports, Science, and Technology and the Ministry of Health, Labor and Welfare, Japan. The study design was approved by the ethics committee of the host institution. Between 1990 and 2006, a total of 2386 patients with HCC were admitted to the University of Tokyo Hospital. A diagnosis of HCC was confirmed radiologically by hyperattenuation in the arterial phase and washout in the late phase using either contrast-enhanced computed tomography (CT) or magnetic resonance imaging (MRI).[18] Ultrasound-guided tumor biopsies were performed when the diagnostic imaging results were inconclusive. In the current analysis, the follow-up period ended on the date of death or on December 31, 2008. Among the 2386 patients in the total HCC cohort in our hospital, extrahepatic metastases were noted in 28 patients at first hospitalization. In addition, extrahepatic metastases were detected in other 314 patients during follow-up observation. Therefore, we retrospectively analyzed 342 patients in our current study.

Diagnosis of Extrahepatic Metastasis and Evaluation of Intrahepatic Lesions

Screenings for extrahepatic metastases were not performed as part of the routine check-up. Most intra-abdominal metastases were detected on abdominal ultrasonography, CT, or MRI studies that were obtained every 3 to 4 months to evaluate intrahepatic lesions. Pulmonary lesions often were noted on chest x-rays, which were obtained routinely at each admission. Additional examinations, such as bone x-ray, bone scintigraphy, and brain CT or MRI studies, were indicated when symptoms attributable to extrahepatic metastasis appeared. These examinations also were undertaken when the HCC-specific tumor markers α-fetoprotein (AFP), lens culinaris agglutinin-reactive fraction of AFP (AFP-L3), or des-γ-carboxy prothrombin (DCP) were elevated and the elevation could not be accounted for by status of the intrahepatic lesion. A diagnosis of extrahepatic metastasis from HCC was based on the enhancement pattern observed on contrast-enhanced CT/MRI studies. Positron emission tomography/CT studies were not obtained routinely, because they were not covered by insurance in Japan. When tumor resections were performed, pathologic investigations also were undertaken. Extrahepatic metastasis detected only at autopsy was not considered an event in this study, because we focused primarily on the diagnosis and treatment of this condition in living patients.

We also evaluated viable intrahepatic lesions at the diagnosis of extrahepatic metastasis by using contrast-enhanced CT/MRI. Post-treatment lesions were not considered viable if they were not enhanced by contrast medium. In the current study, vascular invasion was diagnosed radiologically, indicating *macroscopic vascular invasion*. Vascular invasion included invasion to the portal vein, hepatic vein, inferior vena cava, and bile duct.

Treatment Responses in Patients With Extrahepatic Metastasis

In principle, treatment responses were evaluated according to Response Evaluation Criteria in Solid Tumors (RECIST) guidelines.[19] A complete response (CR) was defined as the disappearance of both intrahepatic lesion and extrahepatic metastasis. In addition, we defined a CR as the disappearance of all intratumoral arterial enhancement according to a recently proposed, modified RECIST assessment for HCC.[20] The evaluation was based on imaging results that were obtained at 2 months after the initiation of treatment. CR was confirmed by repeat assessments performed ≥4 weeks after the criteria for response first were met.

Statistical Procedures

Survival after diagnosis of extrahepatic metastases was defined as the interval from the date of diagnosis to the date of death from any cause or to the last visit before